

Advances Detector Technologies 1/3

CERN Fermilab Hadron Collider Physics Summer School

Werner Riegler, CERN, werner.riegler@cern.ch

Sept 3rd , 2019

History of Particle Physics

- 1895: X-rays, W.C. Röntgen
- 1896: Radioactivity, H. Becquerel
- 1899: Electron, J.J. Thomson
- 1911: Atomic Nucleus, E. Rutherford
- 1919: Atomic Transmutation, E. Rutherford
- 1920: Isotopes, E.W. Aston
- 1920-1930: Quantum Mechanics, Heisenberg, Schrödinger, Dirac
- 1932: Neutron, J. Chadwick
- 1932: Positron, C.D. Anderson
- 1937: Mesons, C.D. Anderson
- 1947: Muon, Pion, C. Powell
- 1947: Kaon, Rochester
- 1950: QED, Feynman, Schwinger, Tomonaga
- 1955: Antiproton, E. Segre
- 1956: Neutrino, Rheines
- etc. etc. etc.

History of Instrumentation

- 1906: Geiger Counter, H. Geiger, E. Rutherford
- 1910: Cloud Chamber, C.T.R. Wilson
- 1912: Tip Counter, H. Geiger
- 1928: Geiger-Müller Counter, W. Müller
- 1929: Coincidence Method, W. Bothe
- 1930: Emulsion, M. Blau
- 1940-1950: Scintillator, Photomultiplier
- 1952: Bubble Chamber, D. Glaser
- 1962: Spark Chamber
- 1968: Multi Wire Proportional Chamber, C. Charpak
- Etc. etc. etc.

On Tools and Instrumentation

“New directions in science are launched by new tools much more often than by new concepts.

The effect of a concept-driven revolution is to explain old things in new ways.

The effect of a tool-driven revolution is to discover new things that have to be explained”

From Freeman Dyson ‘Imagined Worlds’



Physics Nobel Prices for Instrumentation

- 1927: C.T.R. Wilson, Cloud Chamber
- 1939: E. O. Lawrence, Cyclotron & Discoveries
- 1948: P.M.S. Blacket, Cloud Chamber & Discoveries
- 1950: C. Powell, Photographic Method & Discoveries
- 1954: Walter Bothe, Coincidence method & Discoveries
- 1960: Donald Glaser, Bubble Chamber
- 1968: L. Alvarez, Hydrogen Bubble Chamber & Discoveries
- 1992: Georges Charpak, Multi Wire Proportional Chamber

All Nobel Price Winners related to the Standard Model: 89 !

(biased personal statistics by W. Riegler

http://www.nobelprize.org/nobel_prizes/physics/)

- 31 for Standard Model Experiments
- 13 for Standard Model Instrumentation and Experiments
- 3 for 'Standard Model Instrumentation'
- 23 for Standard Model Theory
- 9 for Quantum Mechanics Theory
- 9 for Quantum Mechanics Experiments
- 1 for Relativity

56 for Experiments and Instrumentation
33 for Theory

The 'Real' World of Particles

ON UNITARY REPRESENTATIONS OF THE INHOMOGENEOUS LORENTZ GROUP*

By E. WIGNER

(Received December 22, 1937)

of the invariance of the transition probability we have

$$(1) \quad |(\varphi_1, \psi_1)|^2 = |(\varphi_{1'}, \psi_{1'})|^2$$

and it can be shown⁴ that the aforementioned constants in the $\varphi_{1'}$ can be chosen in such a way that the $\varphi_{1'}$ are obtained from the φ_1 by a linear unitary operation, depending, of course, on l and l'

$$(2) \quad \varphi_{1'} = D(l', l)\varphi_1.$$

By going over from a first system of reference l to a second $l' = L_1 l$ and then to a third $l'' = L_2 L_1 l$ or directly to the third $l'' = (L_2 L_1)l$, one must obtain—apart from the above mentioned constant—the same set of wave functions. Hence from

$$\varphi_{1''} = D(l'', l')D(l', l)\varphi_1$$

$$\varphi_{1''} = D(l'', l)\varphi_1$$

it follows

$$(3) \quad D(l'', l')D(l', l) = \omega D(l'', l)$$

D. Classification of unitary representations from the point of view of infinitesimal operators

E. Wigner:

“A particle is an irreducible representation of the inhomogeneous Lorentz group”

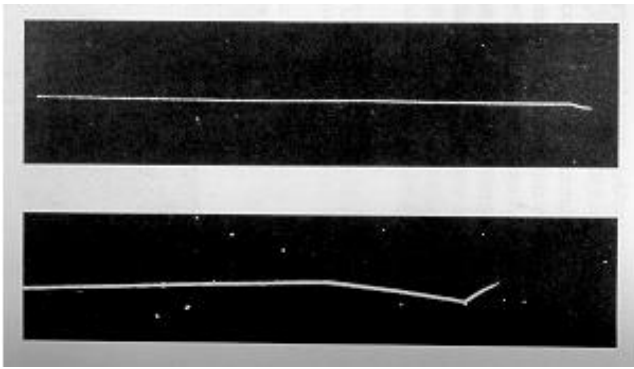
Spin=0, 1/2, 1, 3/2 ...
Mass ≥ 0

E.g. in Steven Weinberg, The Quantum Theory of Fields, Vol1

Particle Detector

W. Riegler:

A particle detector is a classical device, that is collapsing wave functions of quantum mechanical states, which are linear super positions of irreducible representations of the inhomogeneous Lorentz group (Poincare group).



Solvay Conference 1927, Einstein:

“A radioactive sample emits alpha particles in all directions; these are made visible by the method of the Wilson Cloud Chamber. Now, if one associates a spherical wave with each emission process, how can one understand that the track of each alpha particle appears as a (very nearly) straight line “

Born, Heisenberg:

“As soon as such an ionization is shown by the appearance of cloud droplets, in order to describe what happens afterwards one must reduce the wave packet in the immediate vicinity of the drops. One thus obtains a wave packet in the form of a ray, which corresponds to the corpuscular character of the phenomenon.”

According to this reasoning the whole process is described in terms of the interaction of a quantum system (the alpha particle) with a classical measurement apparatus (the atoms of the vapour).

Nevill Mott (1929):

Assuming the atoms of the vapour also to be part of the quantum mechanical system, “ ... it is a little difficult to picture how it is that an outgoing spherical wave can produce a straight track; we think intuitively that it should ionise atoms at random throughout space.”

Mott considers an example with an alpha particle at the origin, one hydrogen atom at position \mathbf{a}_1 and another hydrogen atom at \mathbf{a}_2 , and the two hydrogen atoms only having EM interaction with the alpha particle:

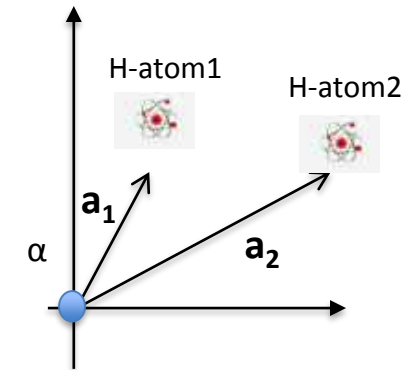


[Mo] Mott N.F., The wave mechanics of α -ray tracks. *Proc. R. Soc. Lond. A*, **126**, 79-84, 1929. Reprinted in: Wheeler J.A., Zurek W., *Quantum Theory and Measurement*, Princeton University Press, 1983.

Main objects of the investigation are periodic solutions $F(\mathbf{R}, \mathbf{r}_1, \mathbf{r}_2)e^{iEt/\hbar}$ of the Schrödinger equation for the three particle system, where \mathbf{R} , \mathbf{r}_1 , \mathbf{r}_2 denote the coordinates of the α -particle and of the two hydrogen atom electrons respectively. The function F (depending parametrically on E) is solution of the stationary Schrödinger equation

$$-\frac{\hbar^2}{2M}\Delta_{\mathbf{R}}F + \left(-\frac{\hbar^2}{2m}\Delta_{\mathbf{r}_1} - \frac{e^2}{|\mathbf{r}_1 - \mathbf{a}_1|}\right)F + \left(-\frac{\hbar^2}{2m}\Delta_{\mathbf{r}_2} - \frac{e^2}{|\mathbf{r}_2 - \mathbf{a}_2|}\right)F - \left(\frac{2e^2}{|\mathbf{R} - \mathbf{r}_1|} + \frac{2e^2}{|\mathbf{R} - \mathbf{r}_2|}\right)F = EF \quad (4.1)$$

where Δ_x is the laplacian with respect to the coordinate x , M is the mass of the α -particle, m is the mass of the electron, $-e$ is the charge of the electron so that $2e$ is the charge of the α -particle.



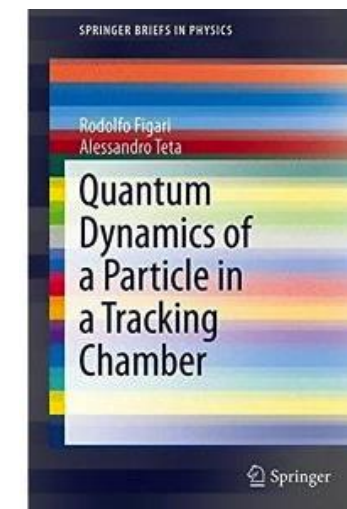
Result: The two hydrogen atoms cannot both be excited (or ionized) unless \mathbf{a}_1 , \mathbf{a}_2 and the origin lie on the same straight line.

(see Also Werner Heisenberg, Chicago lectures 1930)

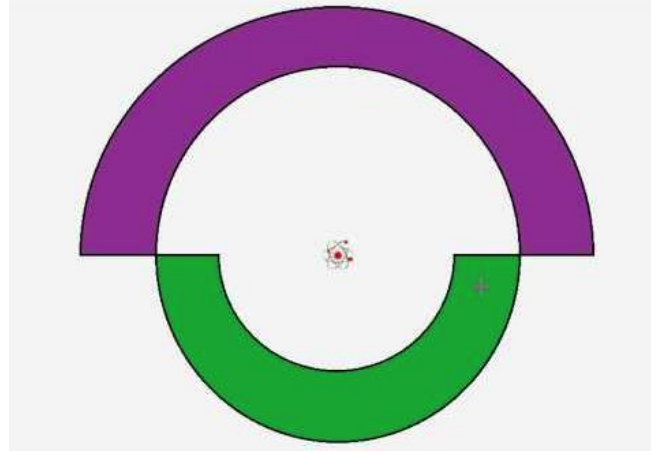
This example (i.e. moving the boundary between the quantum system and classical measurements device) is also used by S. Coleman in the lecture

Quantum Mechanics in Your Face [1994] <https://www.youtube.com/watch?v=EtyNMIXN-sw>

to show how the collapse of the wave function and other 'interpretations of QM' become unnecessary if one removes this boundary and simply considers the entire world (including us) as QM systems.



Renninger's negative-result experiment (1953)



A radioactive atom (emitting an alpha particle) is placed in the center of a detector that consists of two hemispheres and that are 100% efficient to alpha particles.

Considering the second (purple) hemisphere to be very large, the absence of a signal on the green detector after a given time will indicate that the alpha particle will hit the purple detector.

The QM analysis will come out right, with a given probability for the red or the green part to fire and zero probability that both fire.

The semi-classical analysis is however confusing:

The wave-function has collapsed although there was no measurement performed with the green detector ?

A non measurement collapses a wave-function ?

The 'Real' World of Particles

W. Riegler:

“...a particle is an object that interacts with your detector such that you can follow it's track,

it interacts also in your readout electronics and will break it after some time,

and if you a silly enough to stand in an intense particle beam for some time you will be dead ...”

The 'Real' World of Particles

matter particles			guage particles
	1st gen.	2nd gen.	3rd gen.
Q U A R K	u <i>up</i>	c <i>charm</i>	t <i>top</i>
	d <i>down</i>	s <i>strange</i>	b <i>bottom</i>
	ν_e <i>e neutrino</i>	ν_μ <i>μ neutrino</i>	ν_τ <i>τ neutrino</i>
L E P T O N	e <i>electron</i>	μ <i>muon</i>	τ <i>tau</i>
	Strong Force g <i>Gluon</i>		
	Electro-Magnetic Force γ <i>photon</i>		
Weak Force W⁺ W⁻ Z <i>W bosons Z boson</i>			
scalar particle(s) H ? ? ... <i>Higgs</i>			

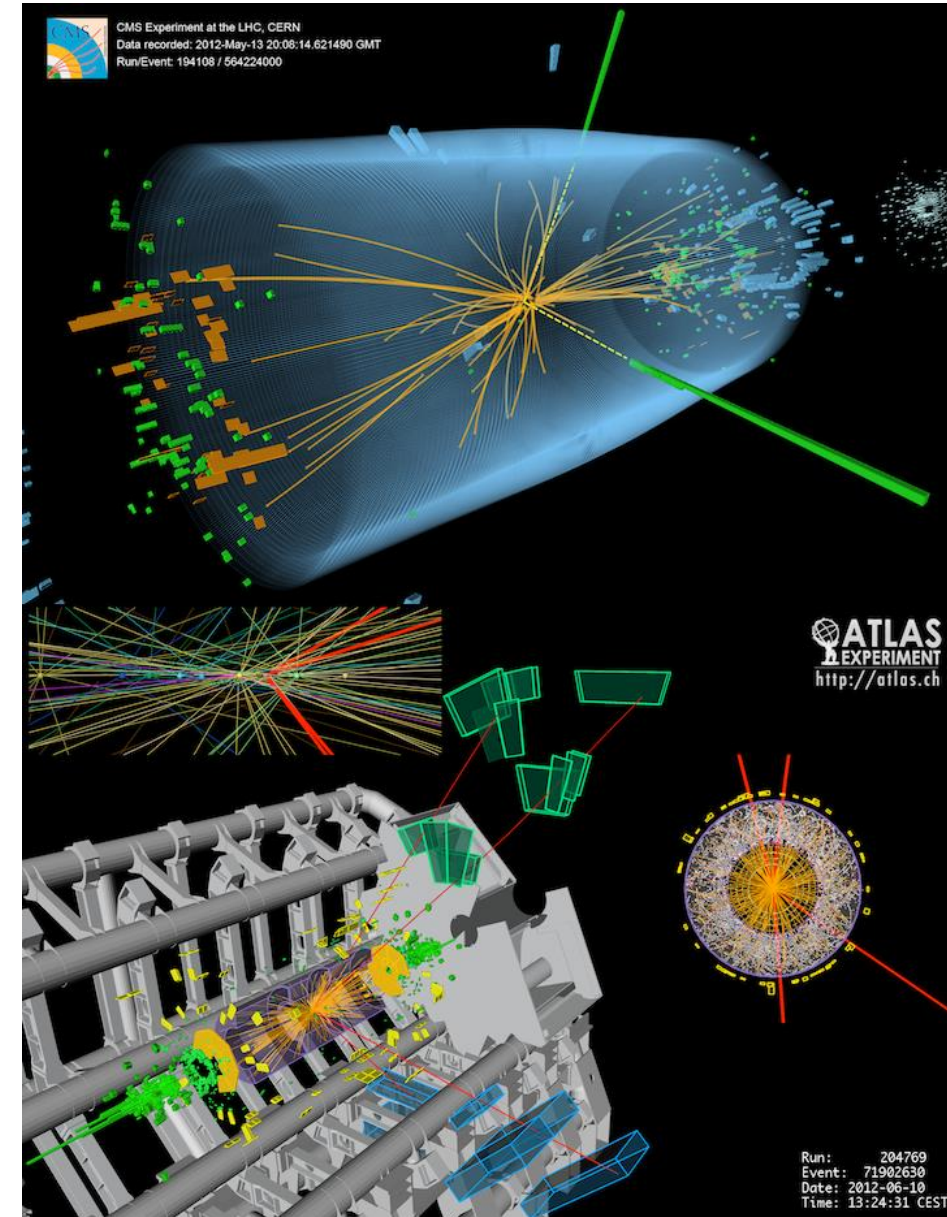
Elektro-Weak Lagrangian

$$L_{GSW} = L_0 + L_H + \sum_l \left\{ \frac{g}{2} \bar{L}_l \gamma_\mu \bar{\tau} L_l \bar{A}^\mu + g' \left[\bar{R}_l \gamma_\mu R_l + \frac{1}{2} \bar{L}_l \gamma_\mu L_l \right] B^\mu \right\} + \frac{g}{2} \sum_q \bar{L}_q \gamma_\mu \bar{\tau} L_q \bar{A}^\mu + g' \left\{ \frac{1}{6} \sum_q \left[\bar{L}_q \gamma_\mu L_q + 4 \bar{R}_q \gamma_\mu R_q \right] + \frac{1}{3} \sum_q \bar{R}_q \gamma_\mu R_q \right\} B^\mu$$

$$L_H = \frac{1}{2} (\partial_\mu H)^2 - m_H^2 H^2 - h \lambda H^3 - \frac{h}{4} H^4 + \frac{g^2}{4} (W_\mu^+ W^\mu + \frac{1}{2 \cos^2 \theta_w} Z_\mu Z^\mu) (\lambda^2 + 2 \lambda H + H^2) + \sum_{l, q, q'} \left(\frac{m_l}{\lambda} \bar{l} l + \frac{m_q}{\lambda} \bar{q} q + \frac{m_{q'}}{\lambda} \bar{q}' q' \right) H$$

Higgs Particle

- Quarks are not seen as free particles, they form Mesons and Baryons, jets at high energies
- Gluons not seen as free particles
- W, Z, H decay 'instantly'
- Neutrinos do not interact in our collider detectors
- ...
- A lot of tricks needed to be invented to 'see' this standard model ...



http://pdg.lbl.gov

~ 180 Selected Particles

$\eta, W^\pm, Z^0, g, e, \mu, \tau, \nu_e, \nu_\mu, \nu_\tau, \pi^\pm, \pi^0, \eta, f_0(660), g(770),$
 $\omega(782), \eta'(958), f_0(980), a_0(980), \phi(1020), h_1(1170), b_1(1235),$
 $a_1(1260), f_2(1270), f_1(1285), \eta(1295), \pi(1300), a_2(1320),$
 $f_0(1370), f_1(1420), \omega(1420), \eta(1440), a_0(1450), g(1450),$
 $f_0(1500), f_2'(1525), \omega(1650), \omega_3(1670), \pi_2(1670), \phi(1680),$
 $g_3(1690), g(1700), f_0(1710), \pi(1800), \phi_3(1850), f_2(2010),$
 $a_4(2040), f_4(2050), f_2(2300), f_2(2340), K^\pm, K^0, K_S^0, K_L^0, K^*(892),$
 $K_1(1270), K_1(1400), K^*(1440), K_0^*(1430), K_2^*(1430), K^*(1680),$
 $K_2(1770), K_3^*(1780), K_2(1820), K_4^*(2045), D^\pm, D^0, D^*(2007),$
 $D^*(2010)^\pm, D_1(2420)^0, D_2^*(2460)^0, D_2^*(2460)^\pm, D_s^\pm, D_s^{*\pm},$
 $D_{s1}(2536)^\pm, D_{s1}(2573)^\pm, B^\pm, B^0, B^*, B_S^0, B_c^\pm, \eta_c(1S), J/\psi(1S),$
 $\chi_{c0}(1P), \chi_{c1}(1P), \chi_{c2}(1P), \psi(2S), \psi(3770), \psi(4040), \psi(4160),$
 $\psi(4415), \Upsilon(1S), \chi_{b0}(1P), \chi_{b1}(1P), \chi_{b2}(1P), \Upsilon(2S), \chi_{b0}(2P),$
 $\chi_{b2}(2P), \Upsilon(3S), \Upsilon(4S), \Upsilon(10860), \Upsilon(11020), p, n, N(1440),$
 $N(1520), N(1535), N(1650), N(1675), N(1680), N(1700), N(1710),$
 $N(1720), N(2190), N(2220), N(2250), N(2600), \Delta(1232), \Delta(1600),$
 $\Delta(1620), \Delta(1700), \Delta(1905), \Delta(1910), \Delta(1920), \Delta(1930), \Delta(1950),$
 $\Delta(2420), \Lambda, \Lambda(1405), \Lambda(1520), \Lambda(1600), \Lambda(1670), \Lambda(1690),$
 $\Lambda(1800), \Lambda(1810), \Lambda(1820), \Lambda(1830), \Lambda(1890), \Lambda(2100),$
 $\Lambda(2110), \Lambda(2350), \Sigma^+, \Sigma^0, \Sigma^-, \Sigma(1385), \Sigma(1660), \Sigma(1670),$
 $\Sigma(1750), \Sigma(1775), \Sigma(1915), \Sigma(1940), \Sigma(2030), \Sigma(2250), \Xi^0, \Xi^-,$
 $\Xi(1530), \Xi(1690), \Xi(1820), \Xi(1950), \Xi(2030), \Omega^-, \Omega(2250)^-,$
 $\Lambda_c^+, \Lambda_c^+, \Sigma_c(2455), \Sigma_c(2520), \Xi_c^+, \Xi_c^0, \Xi_c'^+, \Xi_c'^0, \Xi(2645)$
 $\Xi_c(2780), \Xi_c(2815), \Omega_c^0, \Lambda_b^0, \Xi_b^0, \Xi_b^-, t\bar{t}$

A selection of particles listed by the particle data group.

How can we tell them apart in our detector ?!

There are many more

Out of the hundreds of known particles, these are the only hadrons that have a lifetime long enough to produce a track of $>1\mu\text{m}$ before they decay (at GeV Level).

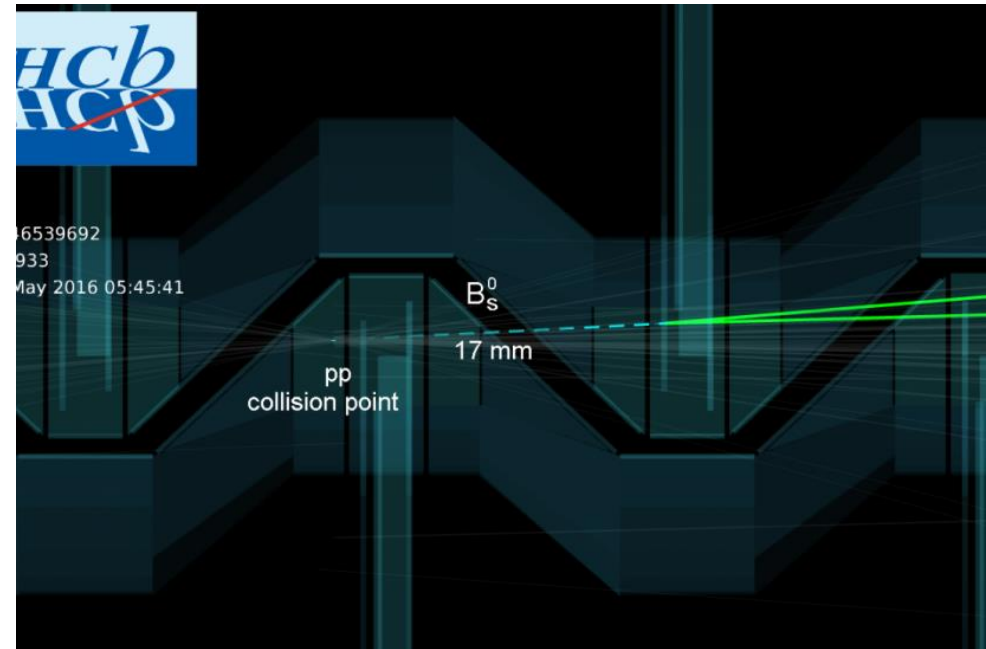
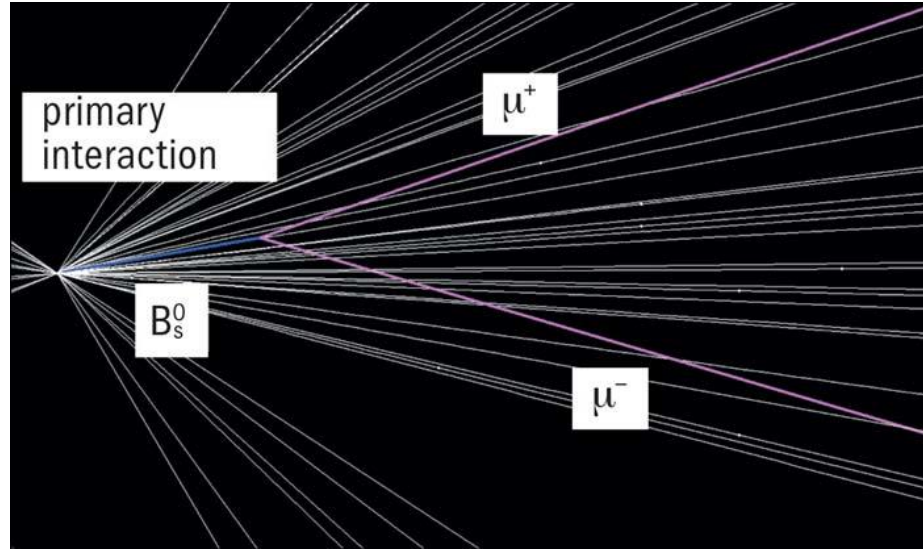
Some of them decay after flying only a few hundred μm .

Others traverse the entire detector.

Particle	Mass (meV)	Life time τ (s)	$c\tau$
$\pi_c^- (u\bar{d}, d\bar{u})$	140	$2.6 \cdot 10^{-8}$	7.8 m
$K^\pm (u\bar{s}, \bar{u}s)$	494	$1.2 \cdot 10^{-8}$	3.7 m
$K^0 (d\bar{s}, \bar{d}s)$	497	$\begin{matrix} 5.1 \cdot 10^{-8} \\ 8.9 \cdot 10^{-11} \end{matrix}$	$\begin{matrix} 15.5 \text{ m} \\ 2.7 \text{ cm} \end{matrix}$
$D^\pm (c\bar{d}, \bar{c}d)$	1869	$1.0 \cdot 10^{-12}$	315 μm
$D^0 (c\bar{u}, \bar{c}u)$	1864	$4.1 \cdot 10^{-13}$	123 μm
$D_s^\pm (c\bar{s}, \bar{c}s)$	1969	$4.9 \cdot 10^{-13}$	147 μm
$B^\pm (u\bar{b}, \bar{u}b)$	5279	$1.7 \cdot 10^{-12}$	502 μm
$B^0 (b\bar{d}, \bar{b}d)$	5279	$1.5 \cdot 10^{-12}$	462 μm
$B_s^0 (s\bar{b}, \bar{s}b)$	5370	$1.5 \cdot 10^{-12}$	438 μm
$B_c^\pm (c\bar{b}, \bar{c}b)$	~ 6400	$\sim 5 \cdot 10^{-13}$	150 μm
$p (uud)$	938.3	$> 10^{33} \text{ y}$	∞
$n (udd)$	939.6	885.7 s	$2.655 \cdot 10^8 \text{ km}$
$\Lambda^0 (uds)$	1115.7	$2.6 \cdot 10^{-10}$	7.89 cm
$\Sigma^+ (uus)$	1189.4	$8.0 \cdot 10^{-11}$	2.404 cm
$\Sigma^- (dds)$	1197.4	$1.5 \cdot 10^{-10}$	4.434 cm
$\Xi^0 (uss)$	1315	$2.9 \cdot 10^{-10}$	8.71 cm
$\Xi^- (dss)$	1321	$1.6 \cdot 10^{-10}$	4.91 cm
$\Omega^- (sss)$	1672	$8.2 \cdot 10^{-11}$	2.461 cm
$\Lambda_c^+ (udc)$	2285	$\sim 2 \cdot 10^{-13}$	60 μm
$\Xi_c^+ (usc)$	2466	$4.4 \cdot 10^{-13}$	132 μm
$\Xi_c^0 (dcs)$	2472	$\sim 1 \cdot 10^{-13}$	29 μm
$\Sigma_c^0 (ssc)$	2698	$6.0 \cdot 10^{-14}$	19 μm
$\Lambda_b (uab)$	5620	$1.2 \cdot 10^{-12}$	368 μm

"Secondary Vertices"

LHCb B decay



From the 'hundreds' of Particles listed by the PDG there are only ~ 27 with a life time $c\tau > \sim 1\mu\text{m}$ i.e. they can be seen as 'tracks' in a Detector.

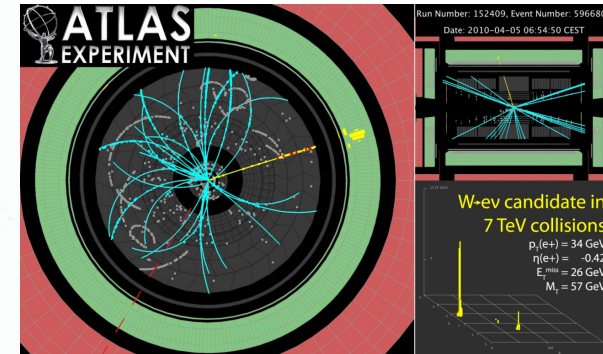
~ 13 of the 27 have $c\tau < 500\mu\text{m}$ i.e. only $\sim\text{mm}$ range at GeV Energies.
 \rightarrow "short" tracks measured with Emulsions or Vertex Detectors.

From the ~ 14 remaining particles

$$e^{\pm}, \mu^{\pm}, \gamma, \pi^{\pm}, K^{\pm}, K^0, p^{\pm}, n$$

are by far the most frequent ones

A particle Detector must be able to identify and measure Energy and Momenta of these 8 particles.

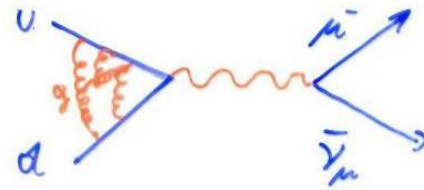


	matter particles			guage particles	
	1st gen.	2nd gen.	3rd gen.		
Q U A R K	u up	c charm	t top	Strong Force g Gluon	
	d down	s strange	b bottom	Electro-Magnetic Force γ photon	
	ν_e e neutrino	ν_μ μ neutrino	ν_τ τ neutrino	Weak Force W⁺ W⁻ Z W bosons Z boson	
L E P T O N	e electron	μ muon	τ tau	scalar particle(s) H Higgs	

Basics:

Two Body Decay

E.g. $\pi^- (ud) \rightarrow \mu^- + \bar{\nu}_\mu$ ($> 99.9\%$)



$$\tau = 2.6 \cdot 10^{-8} \text{ s}$$

π^-
 $\vec{p} = 0, E = m_\pi c^2$

μ^- $\bar{\nu}_\mu$
 $\vec{p}_1 + \vec{p}_2 = 0, E_\mu + E_\nu = E$

$$\begin{aligned} 0 &= \frac{m_\mu v_1}{\sqrt{1 - \frac{v_1^2}{c^2}}} + \frac{m_\nu v_2}{\sqrt{1 - \frac{v_2^2}{c^2}}} \\ m_\pi c^2 &= \frac{m_\mu c^2}{\sqrt{1 - \frac{v_1^2}{c^2}}} + \frac{m_\nu c^2}{\sqrt{1 - \frac{v_2^2}{c^2}}} \end{aligned} \left. \vphantom{\begin{aligned} 0 &= \frac{m_\mu v_1}{\sqrt{1 - \frac{v_1^2}{c^2}}} + \frac{m_\nu v_2}{\sqrt{1 - \frac{v_2^2}{c^2}}} \\ m_\pi c^2 &= \frac{m_\mu c^2}{\sqrt{1 - \frac{v_1^2}{c^2}}} + \frac{m_\nu c^2}{\sqrt{1 - \frac{v_2^2}{c^2}}} \right\} v_1, v_2$$

E_μ, E_ν are uniquely defined

→ Two Body Decay gives "sharp"

Energies of the Decay Particles

Basics:

Three Body Decay

1920ies: β^- Radioactivity



But: e^- shows a continuous Energy Spectrum

→ W. Pauli proposed an "invisible" Particle → $\bar{\nu}$

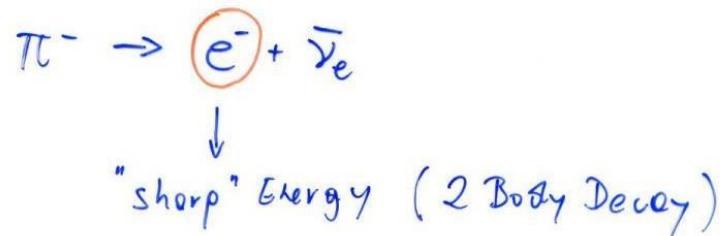
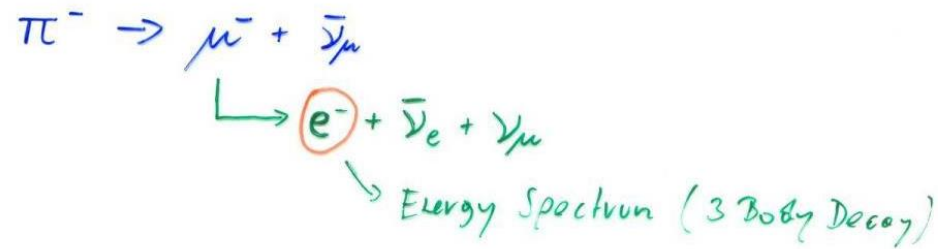
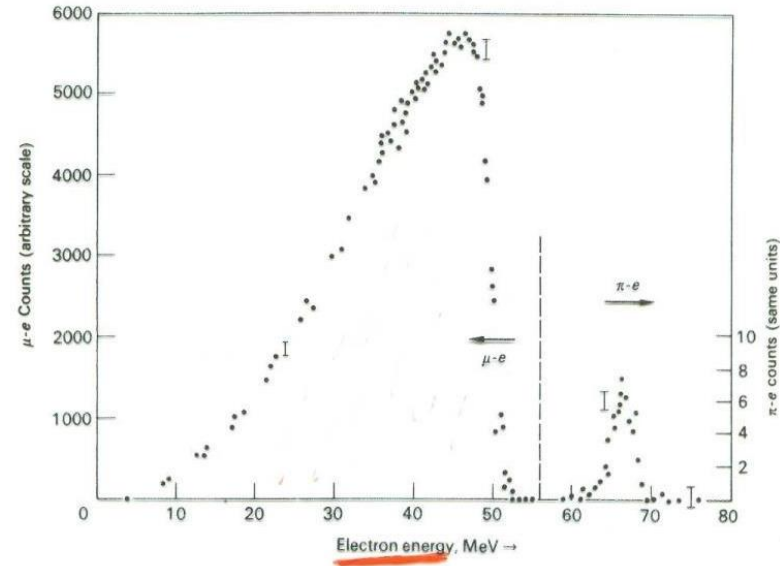


For > 2 Body decay, the Energy Spectrum of the decay particles depends on the Nature of the Interaction. Kinematics alone doesn't define the Energies.

Basics:

Two Body and Three Body Decay

Stopping Pions and measuring the decay electron Spectrum:

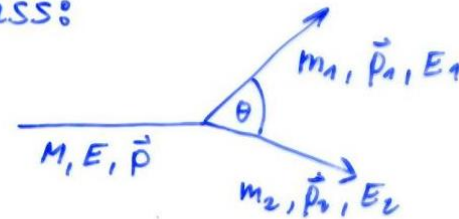


Basics:

Invariant Mass

Invariant Mass:

LAB:



Relativity: $\tilde{a} = \begin{pmatrix} a_0 \\ \vec{a} \end{pmatrix}$ $\tilde{b} = \begin{pmatrix} b_0 \\ \vec{b} \end{pmatrix}$ $\tilde{a} \tilde{b} = a_0 b_0 - \vec{a} \cdot \vec{b}$

$$E = mc^2 \gamma, \quad \vec{p} = m \vec{v} \gamma$$

$$\tilde{p} = \begin{pmatrix} \frac{E}{c} \\ \vec{p} \end{pmatrix}, \quad \tilde{p}_1 = \begin{pmatrix} \frac{E_1}{c} \\ \vec{p}_1 \end{pmatrix}, \quad \tilde{p}_2 = \begin{pmatrix} \frac{E_2}{c} \\ \vec{p}_2 \end{pmatrix}$$

$$\tilde{p} = \tilde{p}_1 + \tilde{p}_2 \quad \text{Energy + Momentum Conservation}$$

$$\tilde{p}^2 = (\tilde{p}_1 + \tilde{p}_2)^2 \rightarrow \tilde{p} \tilde{p} = \tilde{p}_1 \tilde{p}_1 + \tilde{p}_2 \tilde{p}_2 + 2 \tilde{p}_1 \tilde{p}_2$$

$$\underline{M^2 c^2 = m_1^2 c^2 + m_2^2 c^2 + 2 \left(\frac{E_1 E_2}{c^2} - p_1 p_2 \cos \theta \right)}$$

- Measuring Momenta and Energies OR
- Measuring Momenta and identifying Particles gives the Mass of the original Particle

Lifetime of a Particle → Exponential distribution

μ -Lifetime

15

The muon (any unstable Particle) doesn't have an inner 'clock', i.e. nothing that tells it' age.

What is the probability $P(t)dt$ that the muon will decay between time t and $t+dt$ after starting to measure it – independently of how long it lived before ?

Probability p that it decays within the time interval dt after starting to measure = $p = P(0) dt = c_1 dt$.

Probability that it does NOT decay in n time intervals dt but the $(n+1)^{st}$ time interval
= $(1-p)^n p \approx \exp(-n p) p$ with $p = c_1 dt$.

n time intervals of dt means a time of $t = n dt \rightarrow$

Probability that the particle decays between time t and $t+dt = \exp(-c_1 t) c_1 dt = P(t) dt$!

$\rightarrow \underline{P(t) = c_1 e^{-c_1 t}} \rightarrow$ Exponential Distribution

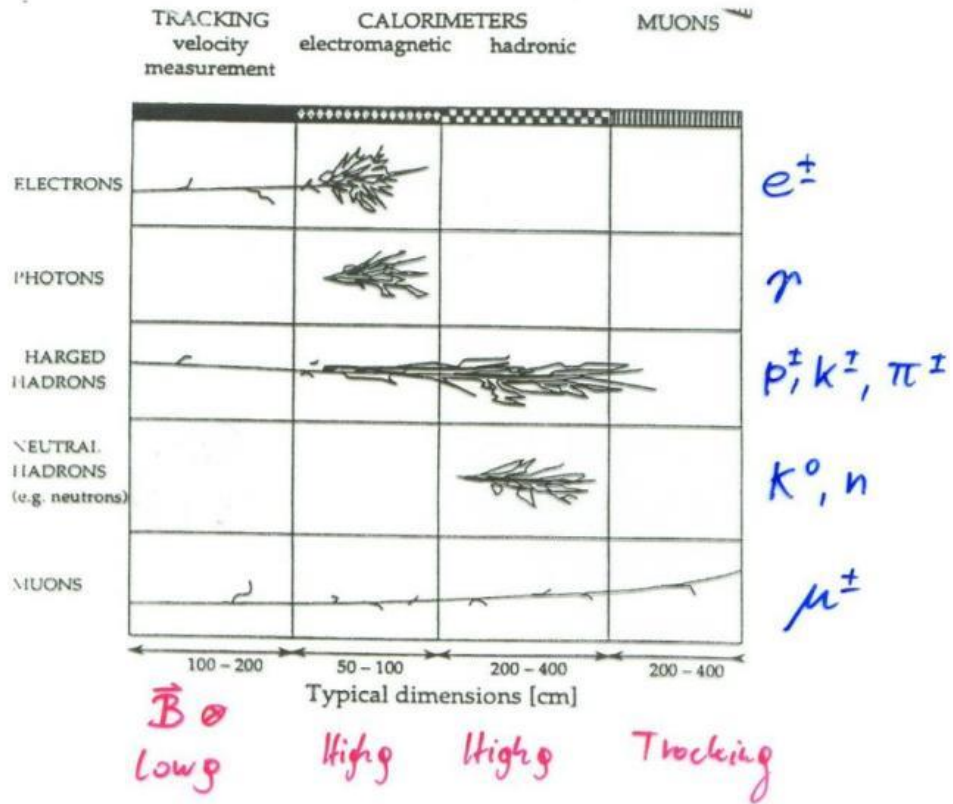
$\gamma = \int_0^{\infty} t c_1 e^{-c_1 t} dt = \frac{1}{c_1}$ Average Lifetime

$P(t) = \frac{1}{\gamma} e^{-\frac{t}{\gamma}}$ $\gamma =$ "Life time"

"A Particle has a lifetime γ " means:

The Probability that it Decays at time t after starting to measure it (independent of what happens before) is $P(t) = \frac{1}{\gamma} e^{-\frac{t}{\gamma}}$

Now that we know all the Interactions we can talk about Detectors !

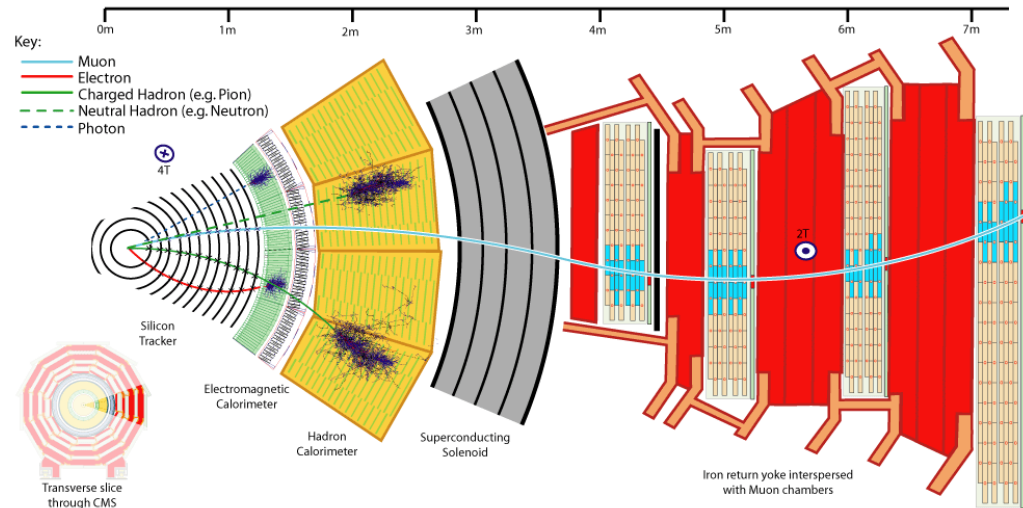


- e^\pm $m_e = 0.511 \text{ MeV}$
 - μ^\pm $m_\mu = 105.7 \text{ MeV} \sim 200 m_e$
 - γ $m_\gamma = 0, Q = 0$
 - π^\pm $m_\pi = 139.6 \text{ MeV} \sim 270 m_e$
 - K^\pm $m_K = 493.7 \text{ MeV} \sim 1000 m_e \sim 3.5 m_\pi$
 - p^\pm $m_p = 938.3 \text{ MeV} \sim 2000 m_e$
 - K^0 $m_{K^0} = 497.7 \text{ MeV} \quad Q = 0$
 - n $m_n = 939.6 \text{ MeV} \quad Q = 0$
- EM, EM, Strong, Strong

Collider Detector

A particle detector is an (almost) irreducible representation of the properties of these 8 particles

$e^{\pm}, \mu^{\pm}, \gamma, \pi^{\pm}, K^{\pm}, K^0, p^{\pm}, n$



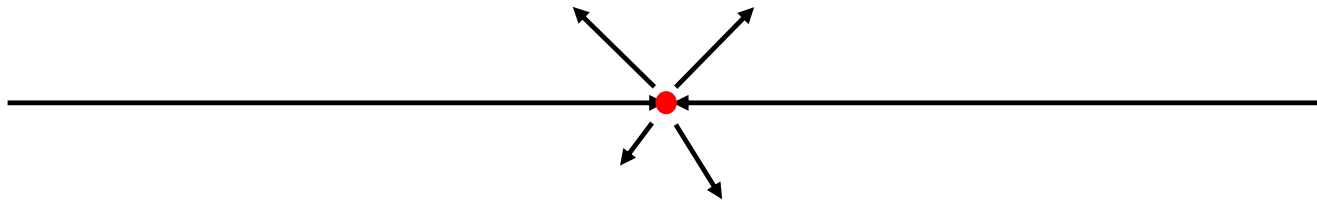
Interaction of Particles with Matter

Any device that is to detect a particle must interact with it in some way → almost ...

In many experiments neutrinos are measured by missing transverse momentum.

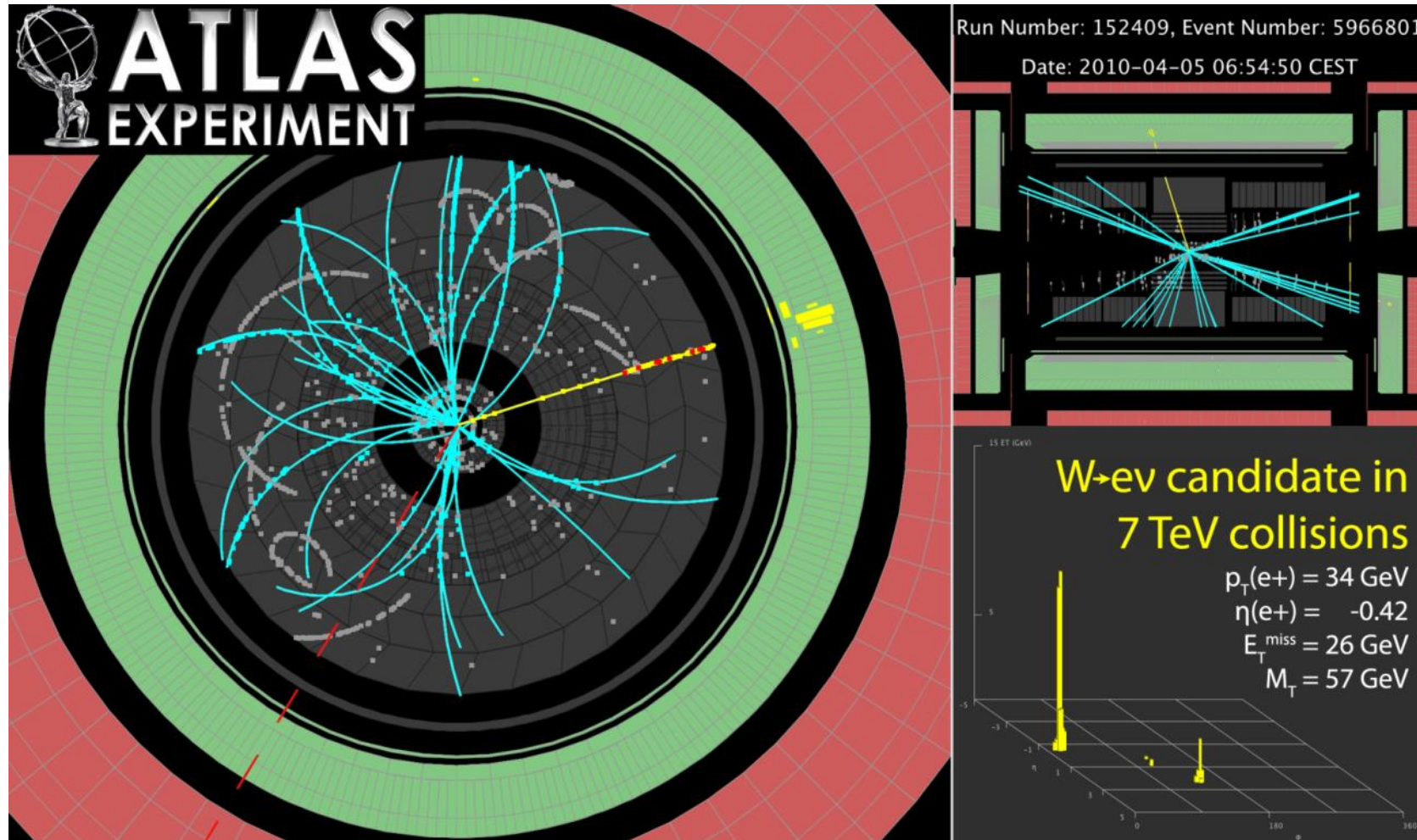
E.g. e^+e^- collider. $P_{\text{tot}}=0$,

If the $\sum p_i$ of all collision products is $\neq 0$ → neutrino escaped.

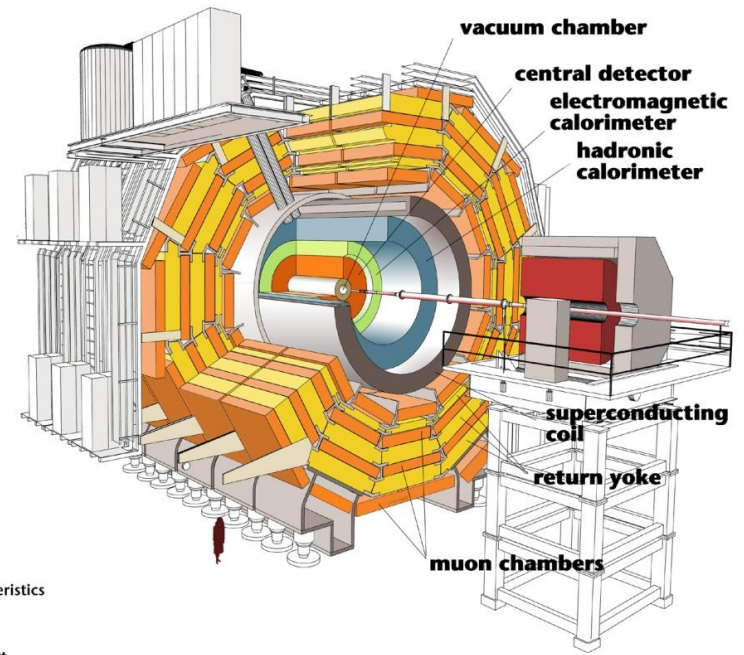
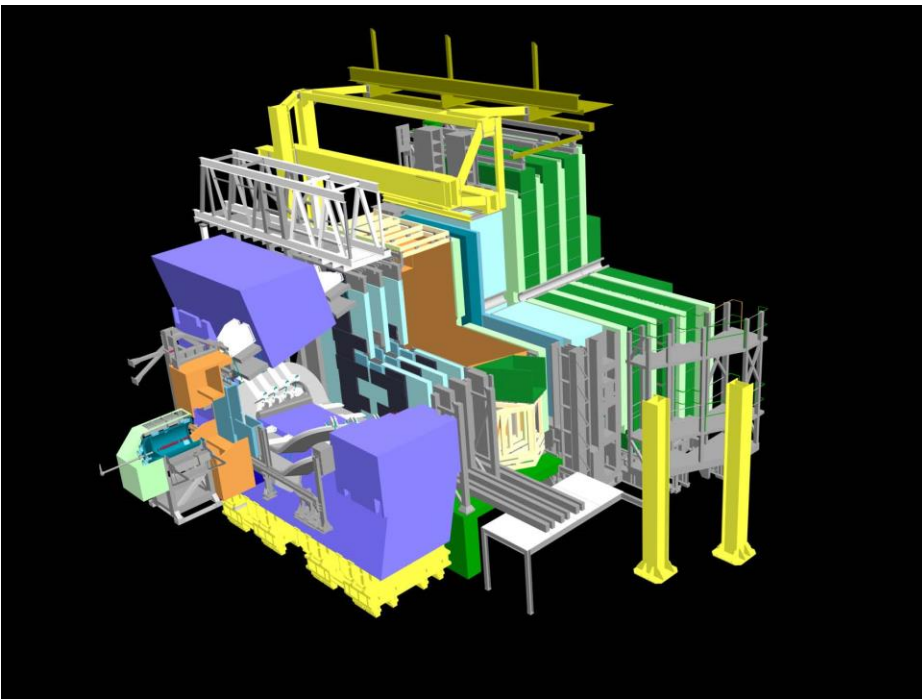
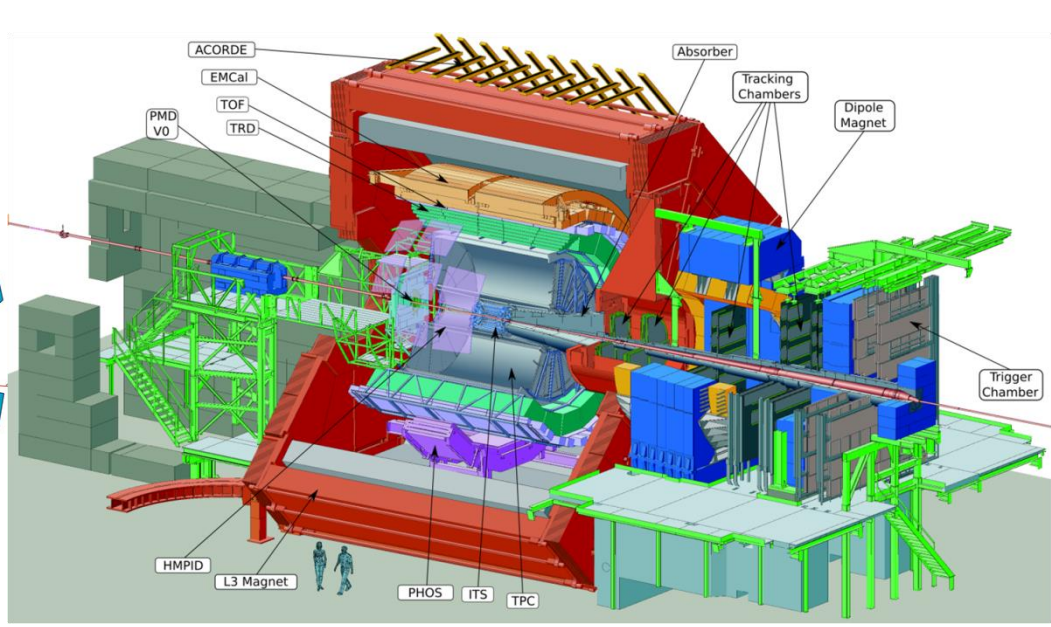
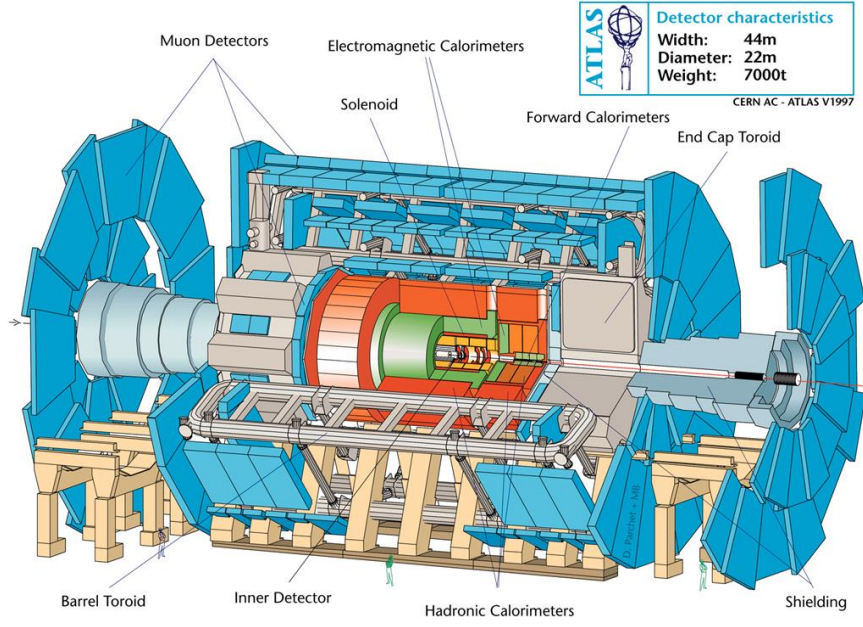


“Did you see it?”
“No nothing.”
“Then it was a neutrino!”

Neutrinos and other invisible particles



They are seen by missing momentum vectors – if you are sure your detector is hermetic !



Detector characteristics
 Width: 22m
 Diameter: 15m
 Weight: 14500t

Principles

Only a few of the numerous known particles have lifetimes that are long enough to leave tracks in a detector.

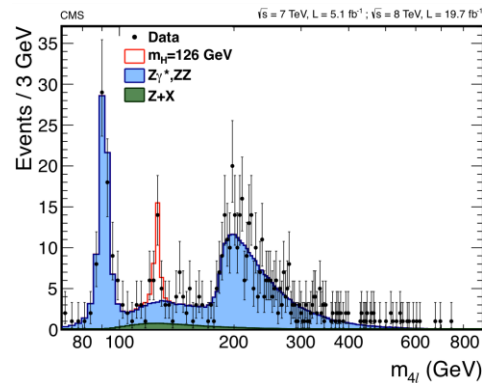
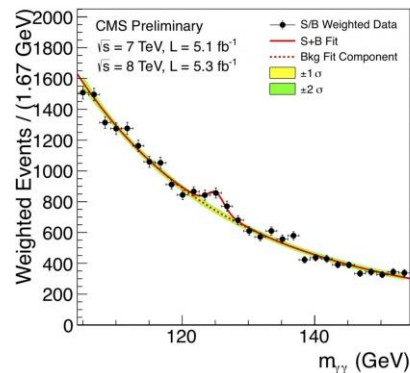
Most of the particles are measured through the decay products and their kinematic relations (invariant mass).

Some short lived particles (b,c –particles) reach lifetimes in the laboratory system that are sufficient to leave short tracks before decaying → identification by measurement of short tracks → secondary vertex tagging

Detectors are built to measure the 8 particles

$e^{\pm}, \mu^{\pm}, \gamma, \pi^{\pm}, K^{\pm}, K^0, p^{\pm}, n$

Their difference in mass, charge and interaction is the key to their identification.



What determines the Size, Material and Geometry of the Detector ?

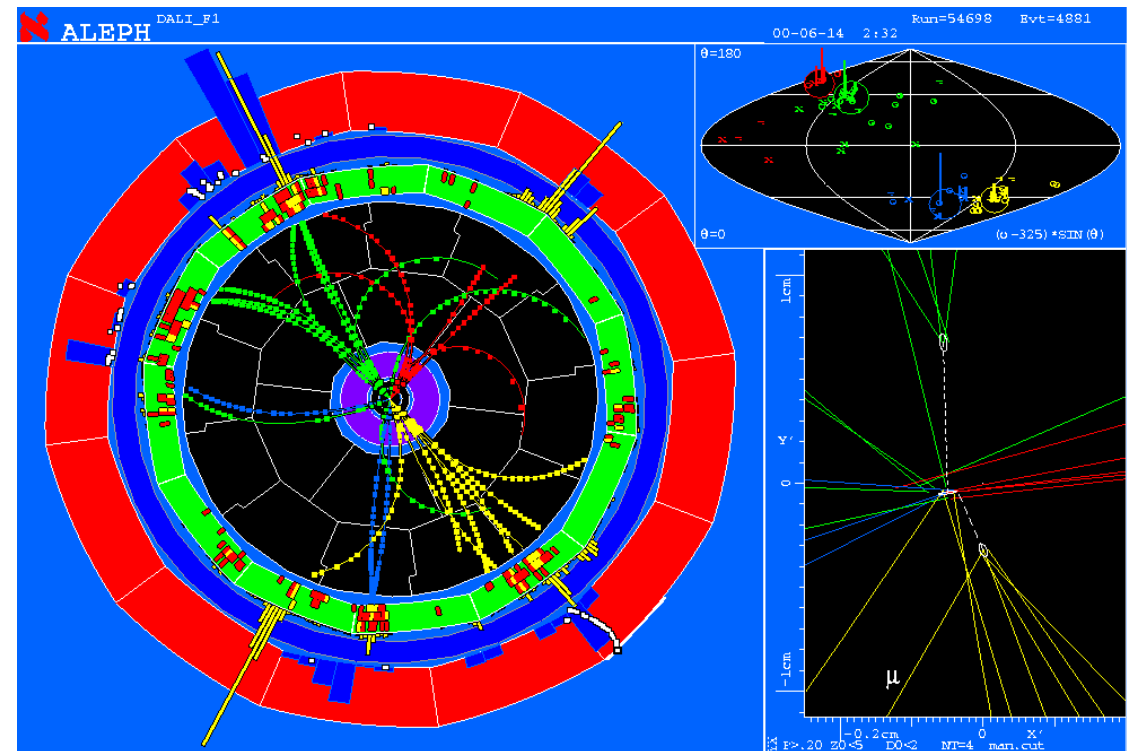
Impact Parameter Measurement (displaced vertices)

Momentum Measurement (bending of tracks in the B-field)

Energy measurement (absorption of particles in the calorimeters)

Muon measurement (identification)

Particle identification and lot's of practical considerations



Multiple Scattering

Statistical (quite complex) analysis of multiple coulomb collisions (Rutherford scattering at the nuclei of the detector material) gives:

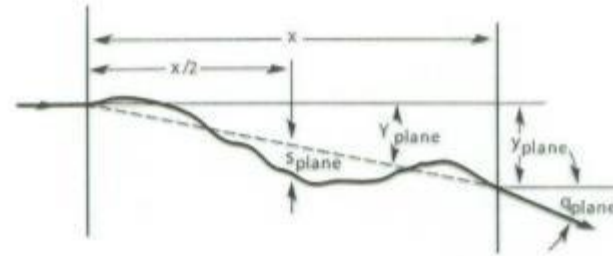
Probability that a particle is deflected by an angle θ after travelling a distance x in the material is given by a Gaussian distribution with sigma of:

$$\Theta_0 = \frac{0.0136}{\beta c p [\text{GeV}/c]} Z_1 \sqrt{\frac{x}{X_0}}$$

X_0 ... Radiation length of the material

Z_1 ... Charge of the particle

p ... Momentum of the particle



$$\sigma(\theta) = \left(\frac{1}{4\pi\epsilon_0}\right)^2 \frac{Z^2 e^4}{M^2 v^4} \times \frac{1}{\sin^4(\theta/2)}$$

Ze = the positive charge of the target atom,
 M = the mass of the α particle,
 v = incident speed of the α particle,
 θ = scattering angle,

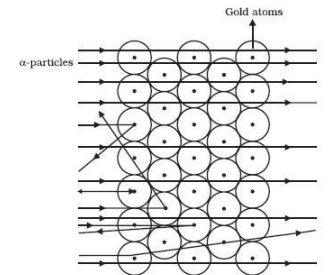


Fig. 4.2: Scattering of α -particles by a gold foil

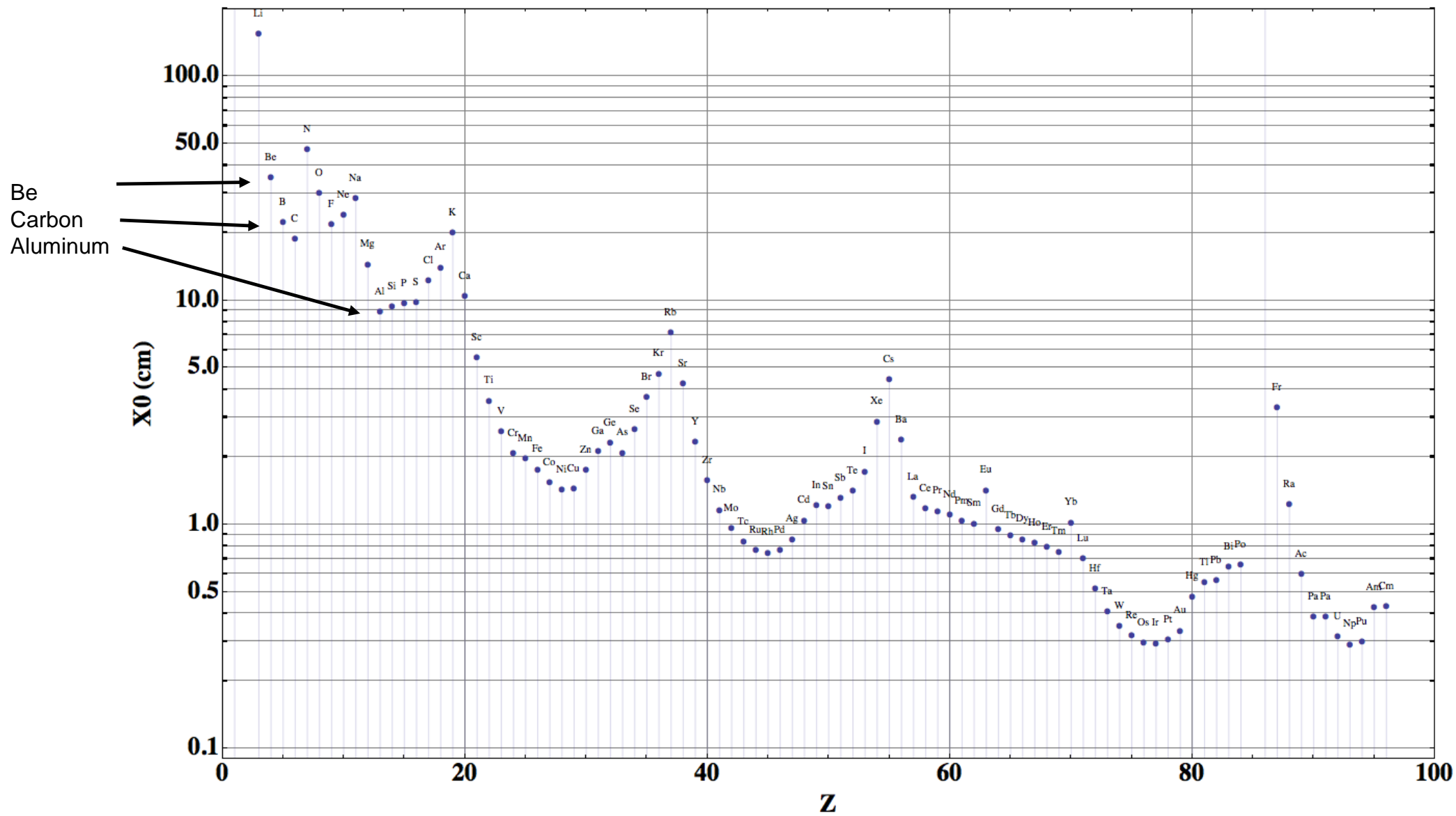
$$E(x) = E_0 e^{-\frac{x}{X_0}} \quad X_0 = \frac{A}{4\pi N_A Z^2 \left(\frac{1}{4\pi\epsilon_0} \frac{e^2}{\hbar c}\right)^2 \ln 183 Z^{-1/3}}$$

For small deflection of the particles by our detector we want:

→ Large Radiation length X_0 – i.e. low Z and low density material (Be, C ...)

→ Small x i.e. very thin detector elements.

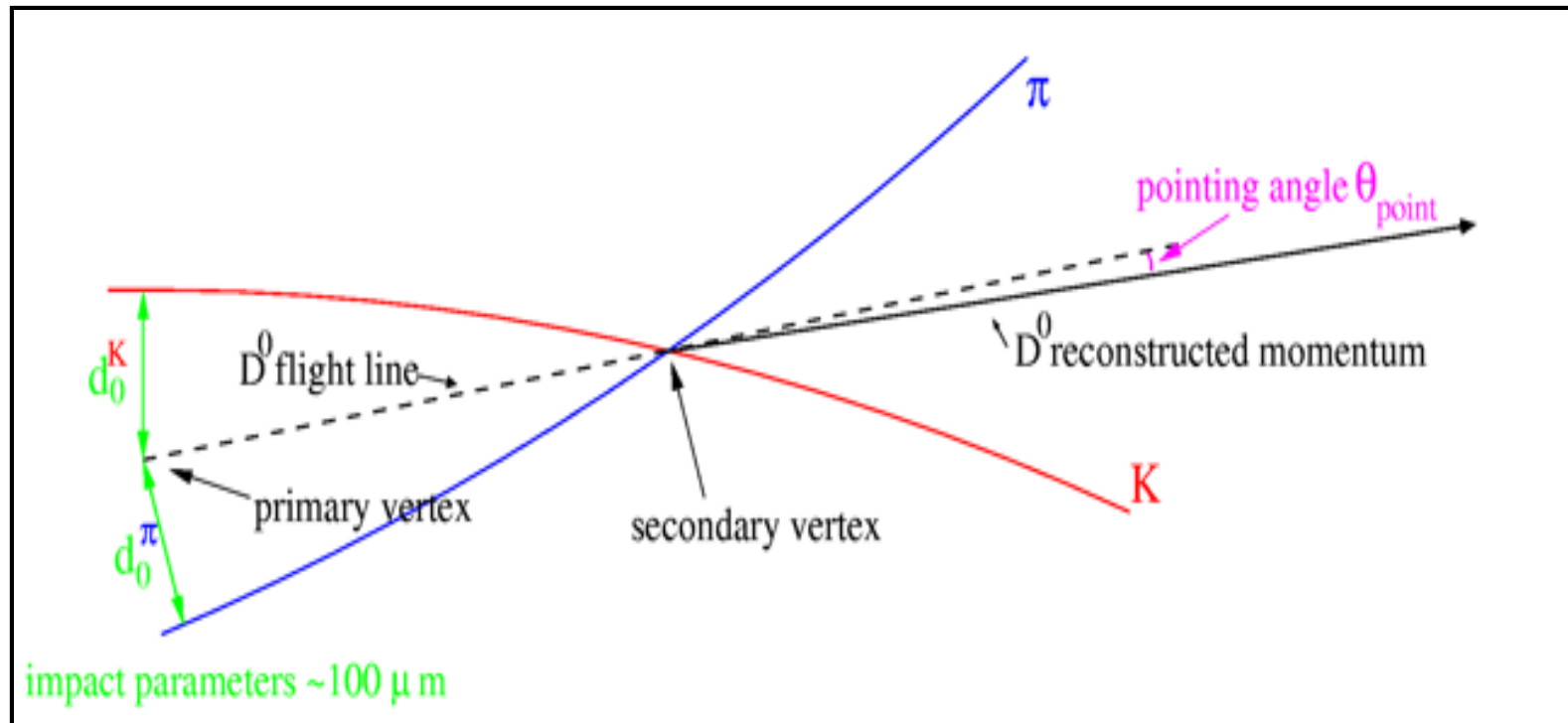
Radiation length of the different elements



Impact Parameter:

Prolongation of a track to the primary vertex. Distance between primary vertex and prolongation is called impact parameter.

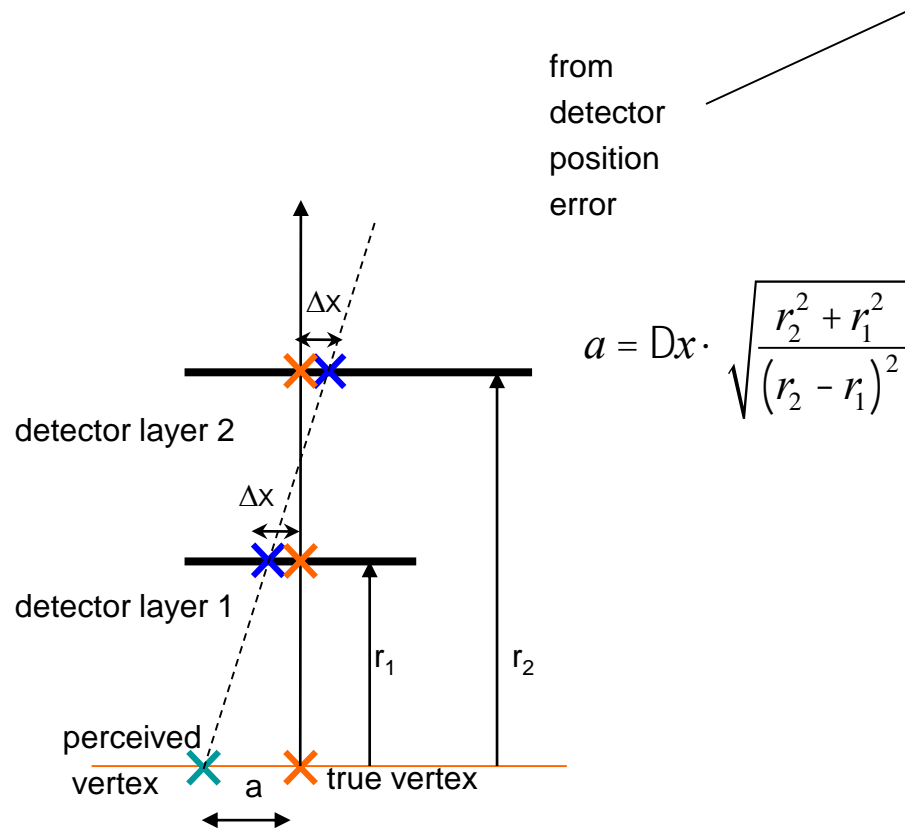
If this number is 'large' the probability is high that the track comes from a secondary vertex.



What determines the impact parameter resolution

Vertex projection from two points: simplified telescope equation

$$\text{pointing resolution} = (a \oplus b) \mu\text{m}$$



Detector Granularity, minimize Δx :

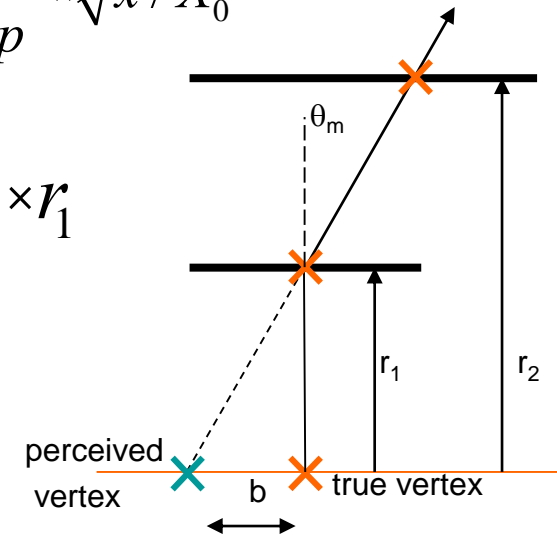
e.g. 50 μm pixel and r_2 very large compared to r_1

$$\rightarrow a = \Delta x = 50 / \sqrt{12} = 15 \mu\text{m}$$

from coulomb scattering

$$q_m = \frac{13.6 \text{ MeV}}{b \times c \times p} \times \sqrt{x / X_0}$$

$$b = q_m \times r_1$$



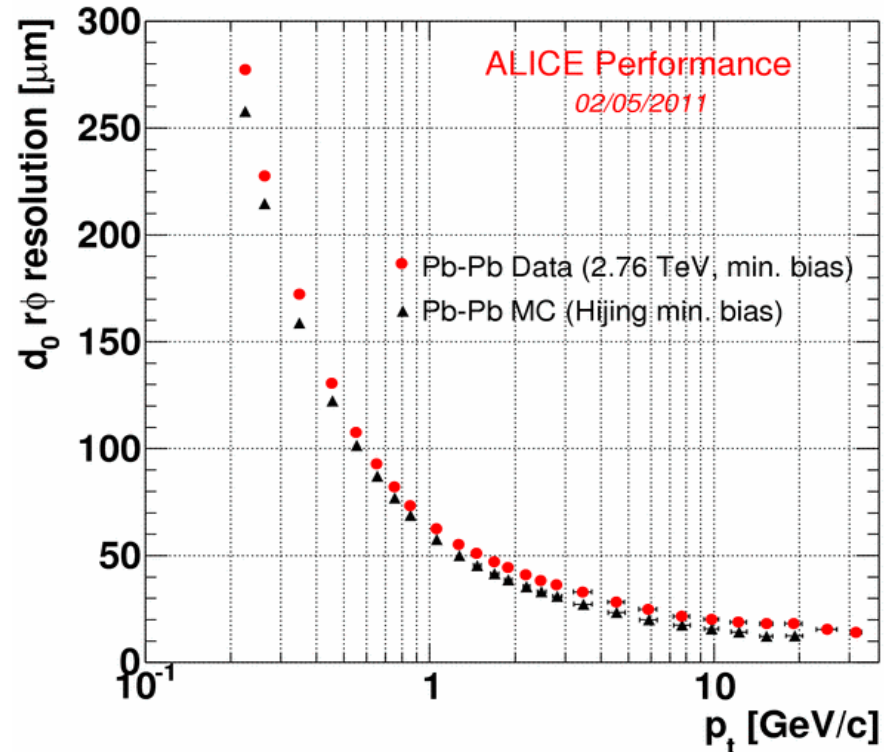
First layer as close as possible to the vertex and First layer with minimal amount of material.

e.g. $x/X_0 = 0.0114$, $r_1 = 39 \text{ mm}$

$$\rightarrow b = 57 \mu\text{m} \text{ for } p = 1 \text{ GeV}/c$$

Example of ALICE Silicon Tracker

Impact parameter resolution



$$a = 15\mu\text{m}$$
$$b = 57\mu\text{m for } p=1\text{GeV}/c$$

For 'low' particle momenta i.e. $p < 10\text{GeV}/c$ the impact parameter resolution is dominated by the material and distance of the first layer.

For high particle momenta the resolution is dominated by the detector granularity.

Alice $x/X_0 = 0.014$ and $r_1 = 39\text{mm}$ is already very good !

Try to improve for upgrade.

Very ambitious goal $x/X_0 = 0.003$ and $r_1 = 22\text{mm}$!

→ Very small beampipe

→ Monolithic silicon sensors $< 50\mu\text{m}$
Optimized carbon fiber supports and cooling tubes.

UNCERTAINTIES IN TRACK MOMENTUM AND DIRECTION, DUE TO MULTIPLE SCATTERING AND MEASUREMENT ERRORS*

R. L. GLUCKSTERN

Physics Department, Yale University, New Haven, Connecticut

Received 23 March 1963

The effect of measurement errors and multiple scattering on the uncertainties in momenta and direction of bubble chamber tracks is reexamined. Results are given for the rms uncertainty in momentum and direction, and their correlation, for uniform weighting, and both uniform spacing and clustering of the measured points. It is shown that for measurement errors, clustering of measured points at the beginning, end, and center of the track leads to lower rms uncertainties. Estimates of the

effect of multiple scattering include the contribution of single and plural small angle scattering outside the central Gaussian region. The contribution of atomic electrons to the multiple scattering is treated separately. In addition the effect of small angle nuclear scattering is included. Some numerical results are presented for a variety of projectiles in liquid hydrogen and propane chambers.

Nuclear Inst. and Methods in Physics Research, A 910 (2018) 127-132



Contents lists available at [ScienceDirect](https://www.sciencedirect.com)

Nuclear Inst. and Methods in Physics Research, A

journal homepage: www.elsevier.com/locate/nima



Explicit formulas for N equal and equidistant detector layers

An extension of the Gluckstern formulae for multiple scattering: Analytic expressions for track parameter resolution using optimum weights



Z. Drasal ^{a,b}, W. Riegler ^{b,*}

^a Charles University, Prague, Czech Republic

^b CERN EP, Geneva, Switzerland

ARTICLE INFO

Keywords:
Tracking
Multiple scattering
Impact parameter resolution
Momentum resolution

ABSTRACT

Momentum, track angle and impact parameter resolution are key performance parameters that tracking detectors are optimised for. This report presents analytic expressions for the resolution of these parameters for equal and equidistant tracking layers. The expressions for the contribution from position resolution are based on the Gluckstern formulae and are well established. The expressions for the contribution from multiple scattering using optimum weights are discussed in detail.

2. General formulae

We assume a particle track of known functional form $f(x) = \sum_{i=0}^M a_i g_i(x)$ with $M + 1$ unknown parameters a_m , and we assume y_n to be the measured positions in the $N + 1$ detector planes placed at x_n . The straight line track in Fig. 3 and the parabolic track in Fig. 4 are the two concrete examples that we will discuss later. The parameters a_i are estimated by minimising χ^2 defined as

$$\chi^2 = \sum_{m=0}^N \sum_{n=0}^N \left[y_m - \sum_{i=0}^M a_i g_i(x_m) \right] W_{mn} \left[y_n - \sum_{i=0}^M a_i g_i(x_n) \right] \quad (1)$$

where W_{mn} is the weight matrix that still has to be defined. The above relation can also be written in matrix form

$$\chi^2 = (\mathbf{y} - \mathbf{G}\mathbf{a})^T \mathbf{W} (\mathbf{y} - \mathbf{G}\mathbf{a}) \quad (2)$$

with $\mathbf{a} = (a_0, a_1, \dots, a_M)$, $\mathbf{y} = (y_0, y_1, \dots, y_N)$ and $G_{mn} = g_n(x_m)$. To minimise χ^2 we have to solve $\partial\chi^2/\partial a_i = 0$ which gives

$$\mathbf{a} = (\mathbf{G}^T \mathbf{W} \mathbf{G})^{-1} \mathbf{G}^T \mathbf{W} \mathbf{y} = \mathbf{B} \mathbf{y} \quad (3)$$

and represents the estimates for the parameters a_i . Next we want to know the variance of these estimated parameters for given measurement errors on y_n . These errors are defined through the covariance matrix \mathbf{C}_y of \mathbf{y} . From error propagation we know that if \mathbf{C}_y is the covariance matrix for \mathbf{y} , the covariance matrix \mathbf{C}_a for $\mathbf{a} = \mathbf{B}\mathbf{y}$ is

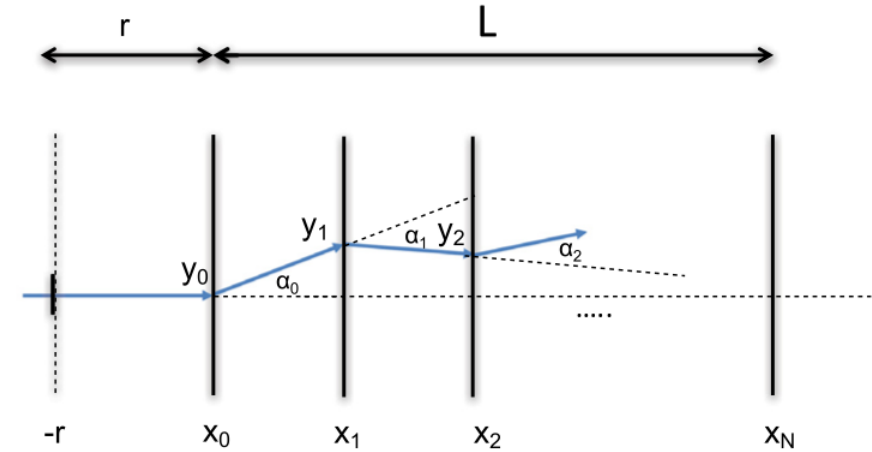
$$\mathbf{C}_a = \mathbf{B} \mathbf{C}_y \mathbf{B}^T = (\mathbf{G}^T \mathbf{W} \mathbf{G})^{-1} \mathbf{G}^T \mathbf{W} \mathbf{C}_y \mathbf{W}^T \mathbf{G} (\mathbf{G}^T \mathbf{W}^T \mathbf{G})^{-1} \quad (4)$$

which is the desired result. The variance of the track position $f(x)$ and track angle $f'(x)$ along the track are then given in analogy by

$$(\Delta f(x))^2 = \mathbf{g}(x)^T \mathbf{C}_a \mathbf{g}(x) \quad (\Delta f'(x))^2 = \mathbf{g}'(x)^T \mathbf{C}_a \mathbf{g}'(x) \quad (5)$$

with $\mathbf{g}(x) = (g_0(x), g_1(x), \dots, g_M(x))$ and $\mathbf{g}'(x) = (g'_0(x), g'_1(x), \dots, g'_M(x))$. The weight matrix \mathbf{W} has to be chosen such that the variances are minimised and the estimators are unbiased. This question is answered by the generalised Gauss–Markov theorem, stating that $\mathbf{W} = \mathbf{C}_y^{-1}$ is the optimum choice. In that case the expression for \mathbf{C}_a reduces to

$$\mathbf{C}_a = (\mathbf{G}^T \mathbf{C}_y^{-1} \mathbf{G})^{-1} \quad (6)$$



$$y_0 = f(x_0) + u_0$$

$$y_1 = f(x_1) + u_1 + \alpha_0(x_1 - x_0)$$

$$y_2 = f(x_2) + u_2 + \alpha_0(x_2 - x_0) + \alpha_1(x_2 - x_1)$$

⋮

$$y_n = f(x_n) + u_n + \sum_{m=0}^{n-1} \alpha_m (x_n - x_m) \quad n = 0, 1, \dots, N$$

The covariance matrix of y_n is therefore

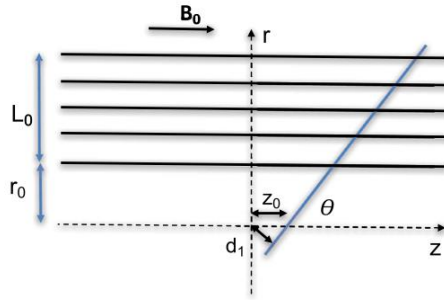
$$(\mathbf{C}_y)_{mn} = \sigma_n^2 \delta_{mn} + \sum_{j=0}^{\text{Min}[m,n]-1} \sigma_{\alpha_j}^2 (x_m - x_j)(x_n - x_j)$$

$$\mathbf{C}_y = \mathbf{R} = \sigma^2 \mathbf{1} \quad \mathbf{C}_y^{-1} = \mathbf{R}^{-1} = \frac{1}{\sigma^2} \mathbf{1} \quad (11)$$

In case multiple scattering dominates we set $\sigma = 0$, and the covariance matrix explicitly reads as

$$\mathbf{C}_y = \mathbf{M} = \frac{\sigma_a^2 L^2}{N^2} \begin{pmatrix} \frac{N^2 \sigma_a^2}{\sigma_a^2 L^2} & 0 & 0 & 0 & 0 & 0 & 0 & 0 & \dots & \dots \\ 0 & 1 & 2 & 3 & 4 & 5 & 6 & 7 & \dots & \dots \\ 0 & 2 & 5 & 8 & 11 & 14 & 17 & 20 & \dots & \dots \\ 0 & 3 & 8 & 14 & 20 & 26 & 32 & 38 & \dots & \dots \\ 0 & 4 & 11 & 20 & 30 & 40 & 50 & 60 & \dots & \dots \\ 0 & 5 & 14 & 26 & 40 & 55 & 70 & 85 & \dots & \dots \\ 0 & 6 & 17 & 32 & 50 & 70 & 91 & 112 & \dots & \dots \\ 0 & 7 & 20 & 38 & 60 & 85 & 112 & 140 & \dots & \dots \\ \vdots & \vdots & \vdots & \vdots & \vdots & \vdots & \vdots & \vdots & \ddots & \ddots \end{pmatrix} \quad (12) \quad \mathbf{C}_y^{-1} = \mathbf{M}^{-1} = \frac{N^2}{\sigma_a^2 L^2} \begin{pmatrix} \frac{L^2 \sigma_a^2}{N^2 \sigma_a^2} & 0 & 0 & 0 & \dots & \dots & \dots & \dots & \dots & \dots \\ 0 & 6 & -4 & 1 & 0 & \dots & \dots & \dots & \dots & \dots \\ 0 & -4 & 6 & -4 & 1 & 0 & \dots & \dots & \dots & \dots \\ 0 & 1 & -4 & 6 & -4 & 1 & 0 & \dots & \dots & \dots \\ \dots & 0 & 1 & -4 & 6 & -4 & 1 & 0 & \dots & \dots \\ \dots & \dots & \dots & \dots & \dots & \dots & \dots & \dots & \dots & \dots \\ \dots & \dots & \dots & \dots & \dots & \dots & \dots & \dots & \dots & \dots \\ \dots & \dots & \dots & \dots & 0 & 1 & -4 & 6 & -4 & 1 & 0 \\ \dots & \dots & \dots & \dots & \dots & 0 & 1 & -4 & 6 & -4 & 1 \\ \dots & \dots & \dots & \dots & \dots & \dots & 0 & 1 & -4 & 5 & -2 \\ \dots & \dots & \dots & \dots & \dots & \dots & \dots & 0 & 1 & -2 & 1 \end{pmatrix}$$

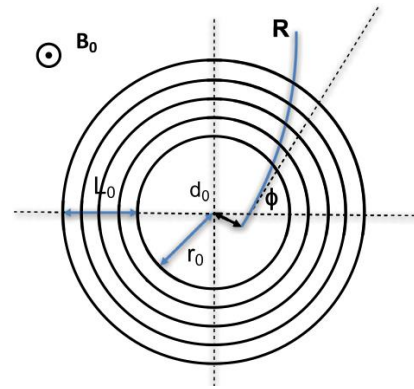
Transverse Impact Parameter Resolution



$$\Delta d_0|_{res.} = \frac{3\sigma_{r\phi}}{\sqrt{(N-1)(N+1)(N+2)(N+3)}} \times \sqrt{\left(N^3 - \frac{N}{3} - \frac{2}{3}\right) + \frac{4(2N^3 - N^2 - N)r_0}{L_0} + \frac{4(7N^3 - N^2 - N)r_0^2}{L_0^2} + \frac{40N^3r_0^3}{L_0^3} + \frac{20N^3r_0^4}{L_0^4}}$$

$$\approx \frac{3\sigma_{r\phi}}{\sqrt{N+5}} \sqrt{1 + \frac{8r_0}{L_0} + \frac{28r_0^2}{L_0^2} + \frac{40r_0^3}{L_0^3} + \frac{20r_0^4}{L_0^4}}$$

Position resolution



$$f(y) = 0.0136 \text{ GeV}/c \times \sqrt{y}(1 + 0.038 \ln y).$$

$$\Delta d_0|_{m.s.} = \frac{r_0}{\beta p_T} f\left(\frac{d}{X_0 \sin \theta}\right) \sqrt{\frac{N-3/4}{N-1} + \frac{N}{2(N-1)} \left(\frac{r_0}{L_0}\right) + \frac{N^2}{4(N-1)} \left(\frac{r_0}{L_0}\right)^2}$$

$$\Delta d_0|_{m.s.}^{opt} = \frac{r_0}{\beta p_T} f\left(\frac{d}{X_0 \sin \theta}\right) \sqrt{1 + \left(\frac{r_0}{L_0}\right) + \left(\frac{r_0}{L_0}\right)^2} \quad N_{opt} = 2 + \frac{L_0}{r_0}$$

$$\approx \frac{0.0136 \text{ GeV}/c}{\beta p_T} r_0 \sqrt{\frac{d}{X_0 \sin \theta}} \sqrt{1 + \left(\frac{r_0}{L_0}\right) + \left(\frac{r_0}{L_0}\right)^2}$$

Multiple scattering

$$\Delta d_0 = a \oplus \frac{b}{p_T \sin^{\frac{1}{2}} \theta} = a \oplus \frac{b \cosh^{\frac{1}{2}} \eta}{p_T}$$

Position resolution

Multiple scattering

For a given

r_0 (distance between the first detector layer and the beamline)

L_0 (tracker radius)

there is an optimum number of layers.

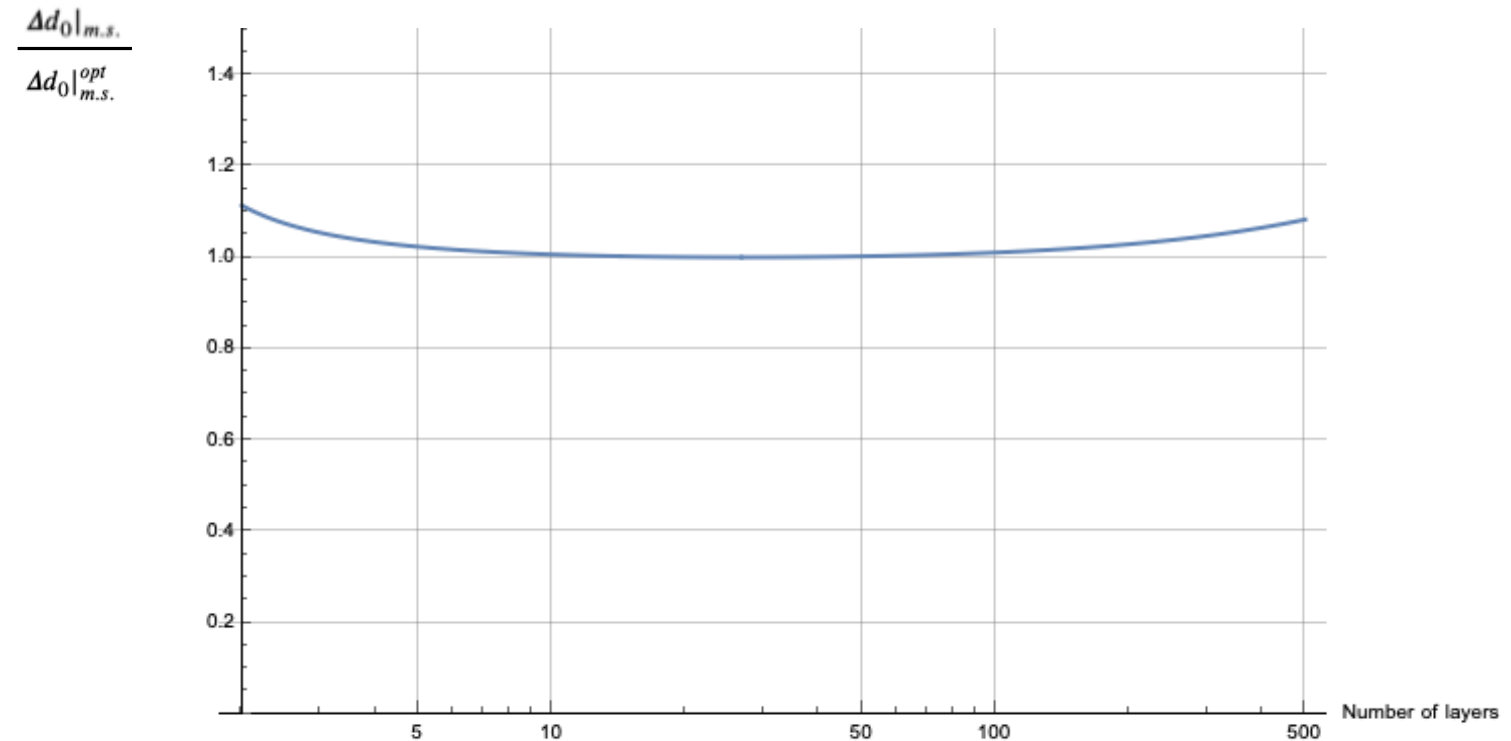
Transverse Impact Parameter Resolution

$r_0=5\text{cm}$, $L_0=125\text{cm}$

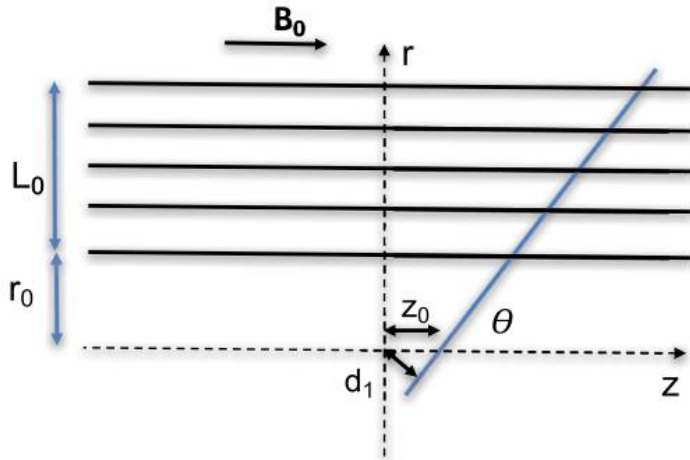
Effect from multiple scattering on d_0 resolution almost independent of number of layers

Another layer gives more information but destroys the new information by the scattering in it's material.

Material budget of the first layer and distance of the first layer to the beampine are the key contributors !



Longitudinal Impact Parameter Resolution



$$\Delta z_0|_{res.} = \frac{2\sigma_z}{\sqrt{(N+1)(N+2)}} \sqrt{\left(N + \frac{1}{2}\right) + \frac{3Nr_0}{L_0} + \frac{3Nr_0^2}{L_0^2}}$$

$$\approx \frac{2\sigma_z}{\sqrt{N+3}} \sqrt{1 + \frac{3r_0}{L_0} + \frac{3r_0^2}{L_0^2}}$$

Position resolution

$$\Delta z_0|_{m.s.} = \frac{r_0}{\sin \theta} \frac{1}{\beta p_T} f\left(\frac{d}{X_0 \sin \theta}\right)$$

$$\approx \frac{0.0136 \text{ GeV}/c}{\beta p_T} \frac{r_0}{\sin \theta} \sqrt{\frac{d}{X_0 \sin \theta}}$$

Multiple scattering

$$\Delta z_0 = a \oplus \frac{b}{p_T \sin^{\frac{3}{2}} \theta} = a \oplus \frac{b \cosh^{\frac{3}{2}} \eta}{p_T}$$

Position resolution

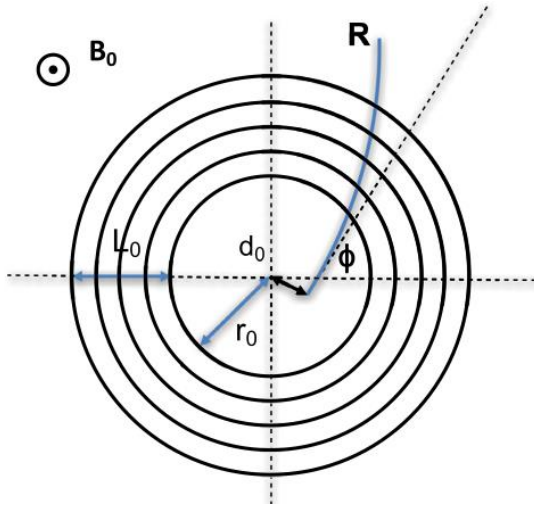
Multiple scattering

M.S. contribution is independent of the number of layers

Two layers as good as any number of layers !

Momentum resolution

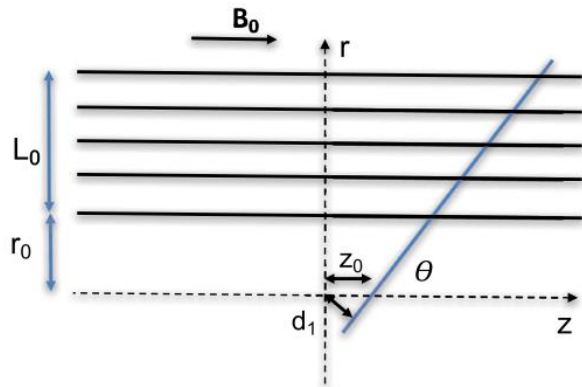
Momentum measurement by measuring the curvature of a track in the B-field



$$\frac{\Delta p_T}{p_T} \Big|_{res.} = \frac{\sigma_{r\phi} p_T}{0.3 B_0 L_0^2} \sqrt{\frac{720 N^3}{(N-1)(N+1)(N+2)(N+3)}}$$

$$\approx \frac{12 \sigma_{r\phi} p_T}{0.3 B_0 L_0^2} \sqrt{\frac{5}{N+5}}$$

Position resolution



$$\frac{\Delta p_T}{p_T} \Big|_{m.s.} = \frac{N}{\sqrt{(N+1)(N-1)}} \frac{0.0136 \text{ GeV}/c}{0.3 \beta B_0 L_0}$$

$$\times \sqrt{\frac{d_{tot}}{X_0 \sin \theta}} \left(1 + 0.038 \ln \frac{d}{X_0 \sin \theta} \right)$$

$$\approx \frac{0.0136 \text{ GeV}/c}{0.3 \beta B_0 L_0} \sqrt{\frac{d_{tot}}{X_0 \sin \theta}}$$

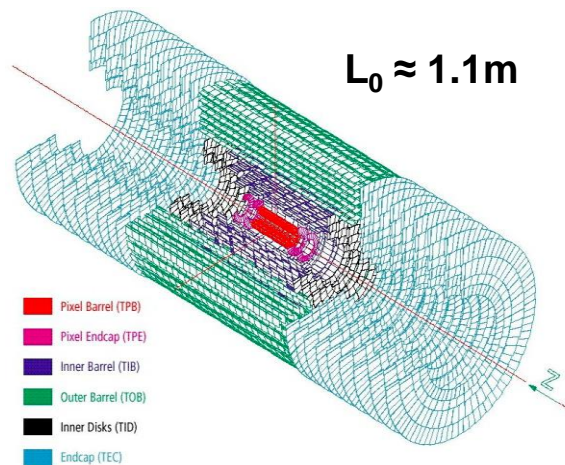
Multiple scattering

$$\frac{\Delta p_T}{p_T} = a p_T \oplus \frac{b}{\sin^{\frac{1}{2}} \theta} \equiv a p_T \oplus b \cosh^{\frac{1}{2}} \eta$$

Position resolution

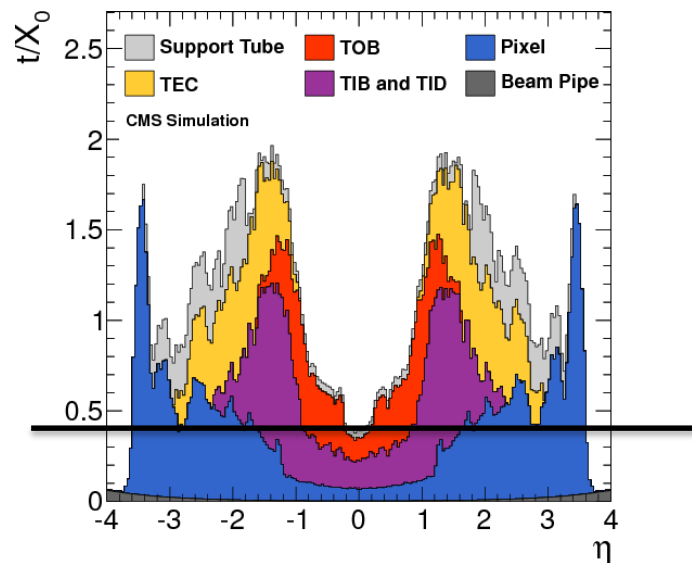
Multiple scattering

Momentum resolution



As an example we use a tracker geometry similar to the CMS experiment, assuming $B_0 = 4\text{T}$, $L_0 = 1.1\text{m}$, $\sigma_{r\phi} = 25\mu\text{m}$, $N + 1 = 14$ and $d_{tot}/X_0 = 0.5$ at $\eta = 0$. This gives $\Delta p_T/p_T|_{m.s.} \approx 0.6\%$, $\sqrt{(\Delta p_T/p_T|_{res.})^2 + (\Delta p_T/p_T|_{m.s.})^2} = 1.2\%$ at $p_T = 100\text{GeV}/c$ as well as $\Delta p_T/p_T|_{res.} = 11\%$ at $p_T = 1000\text{GeV}/c$, which compares well with the numbers quoted in [8].

Material budget



The momentum resolution is dominated by M.S.
Up to $50\text{GeV}/c$ at $\eta=0$
Up to 100GeV in the forward regions

Tracker material is THE essential ingredient to performance !!

Excursion to Silicon Detectors

Silicon trackers are used for vertex measurement in all LHC experiments and for momentum spectroscopy on most LHC experiments (ALICE TPC, LHCb fiber tracker)

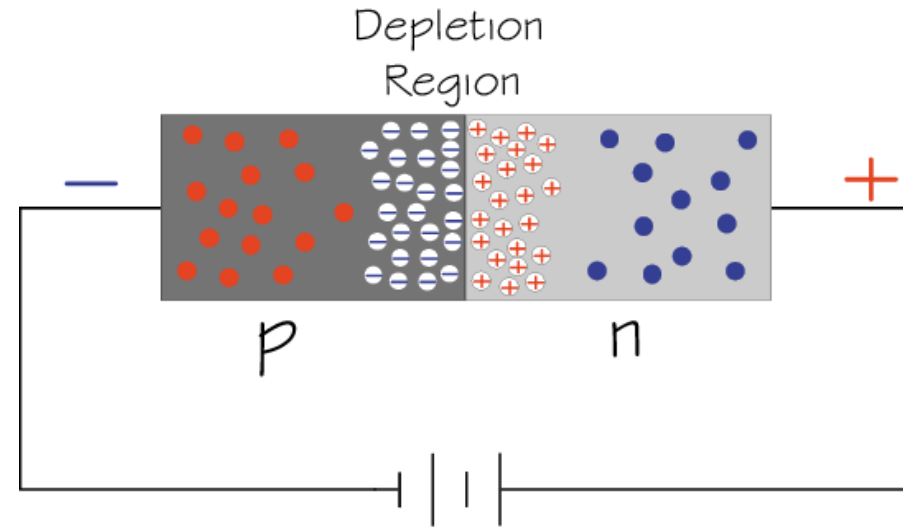
Si-Diode used as a Particle Detector

At the p-n junction the charges are depleted and a zone free of charge carriers is established.

By applying a voltage, the depletion zone can be extended to the entire diode → highly insulating layer.

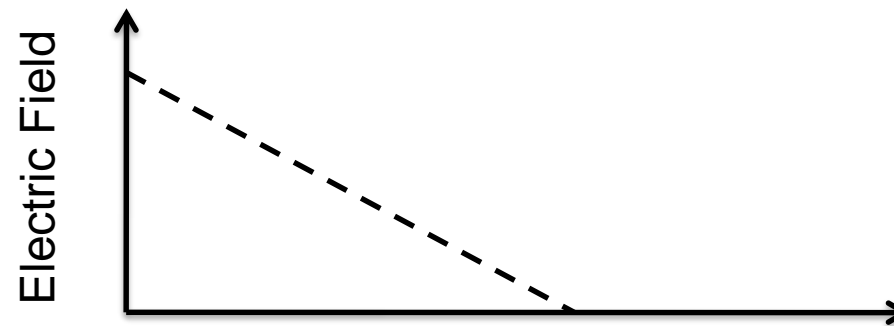
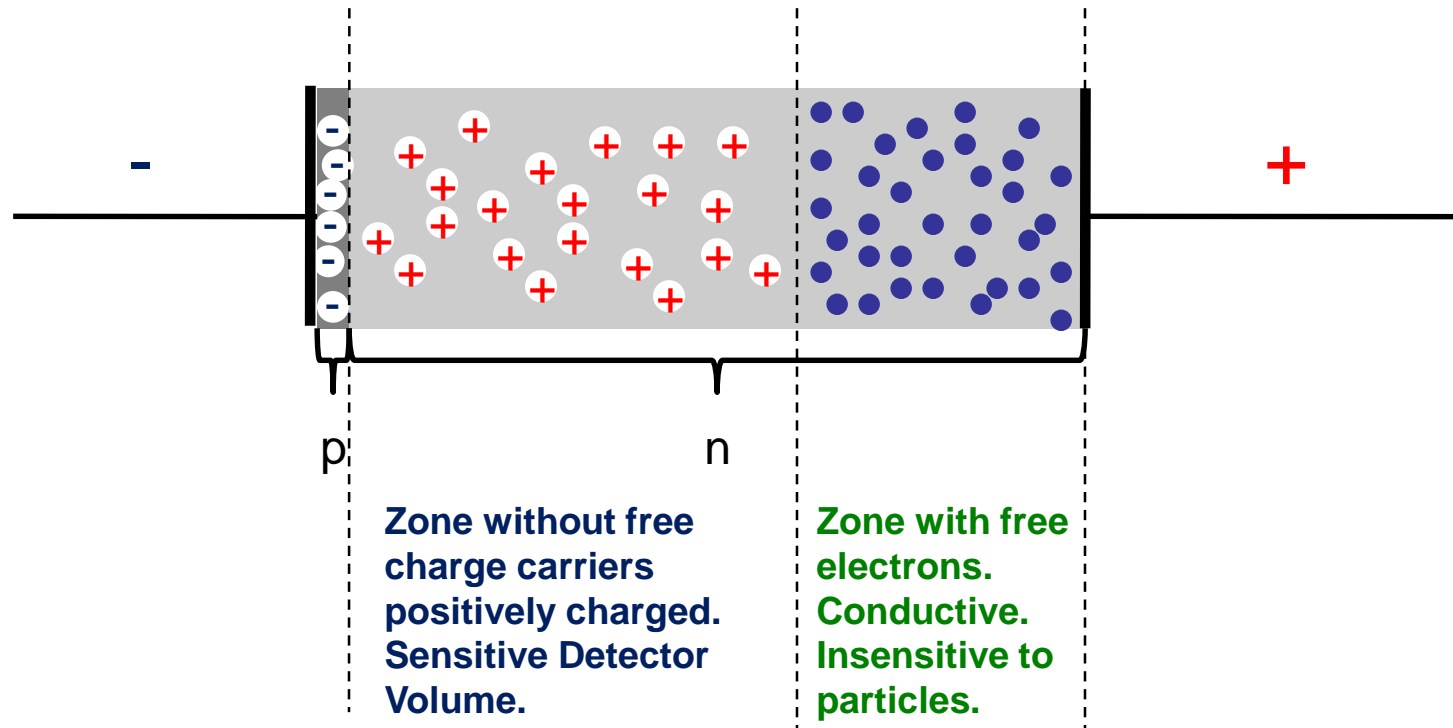
An ionizing particle produces free charge carriers in the diode, which drift in the electric field and induce an electrical signal on the metal electrodes.

As silicon is the most commonly used material in the electronics industry, it has one big advantage with respect to other materials, namely highly developed technology.

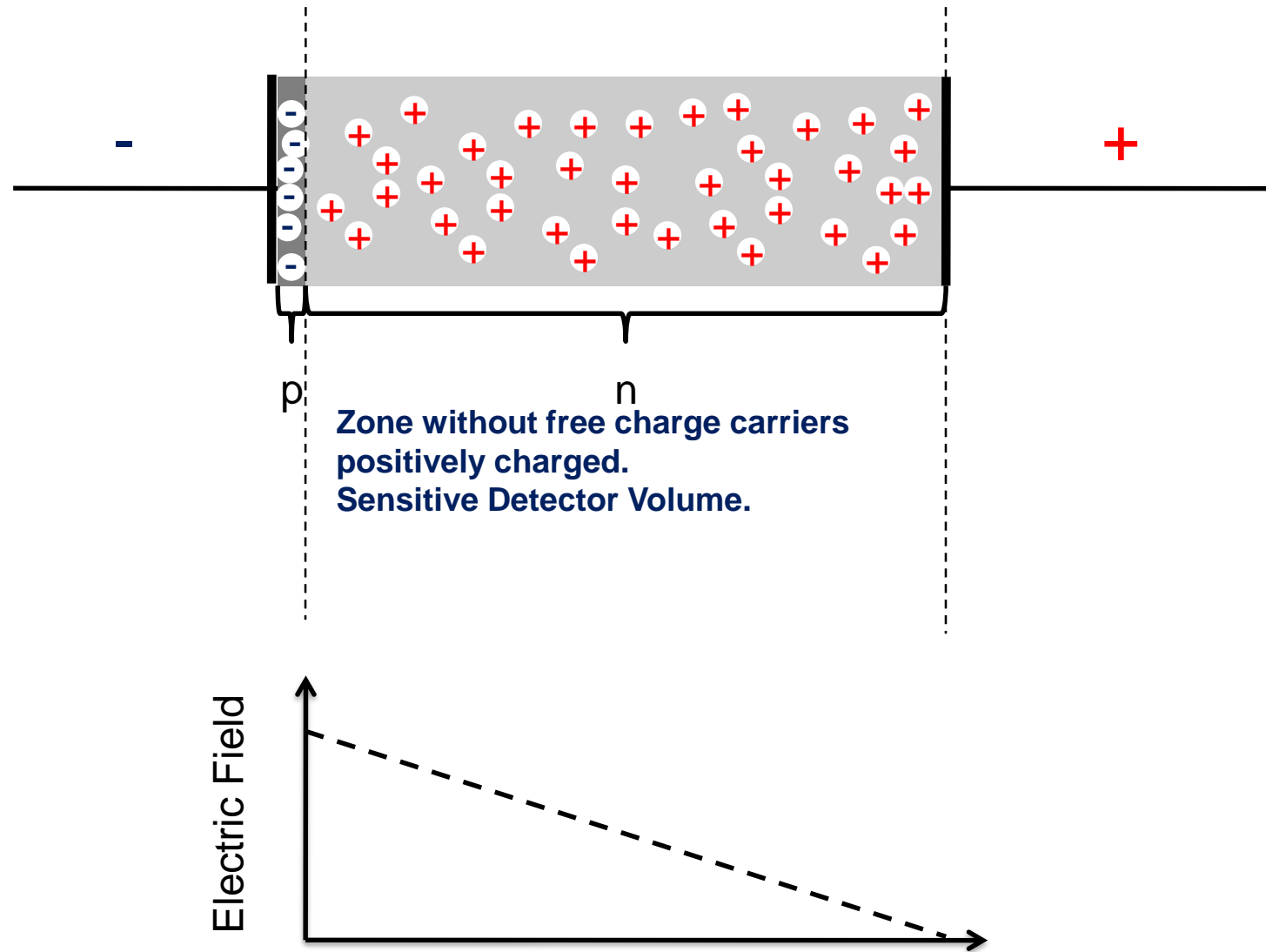


- Electron
- ⊕ Positive ion from removal of electron in n-type impurity
- ⊖ Negative ion from filling in p-type vacancy
- Hole

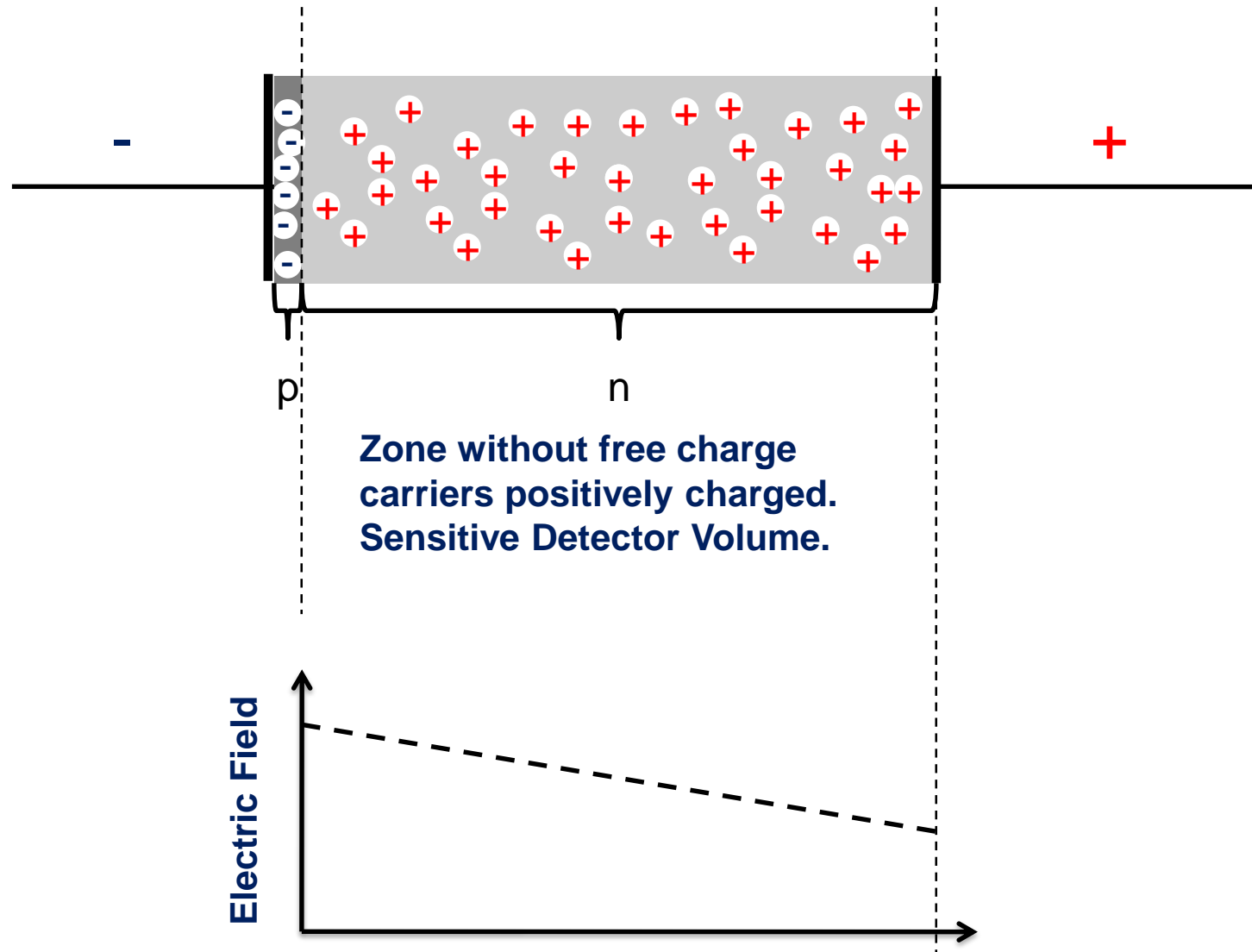
Under-Depleted Silicon Detector



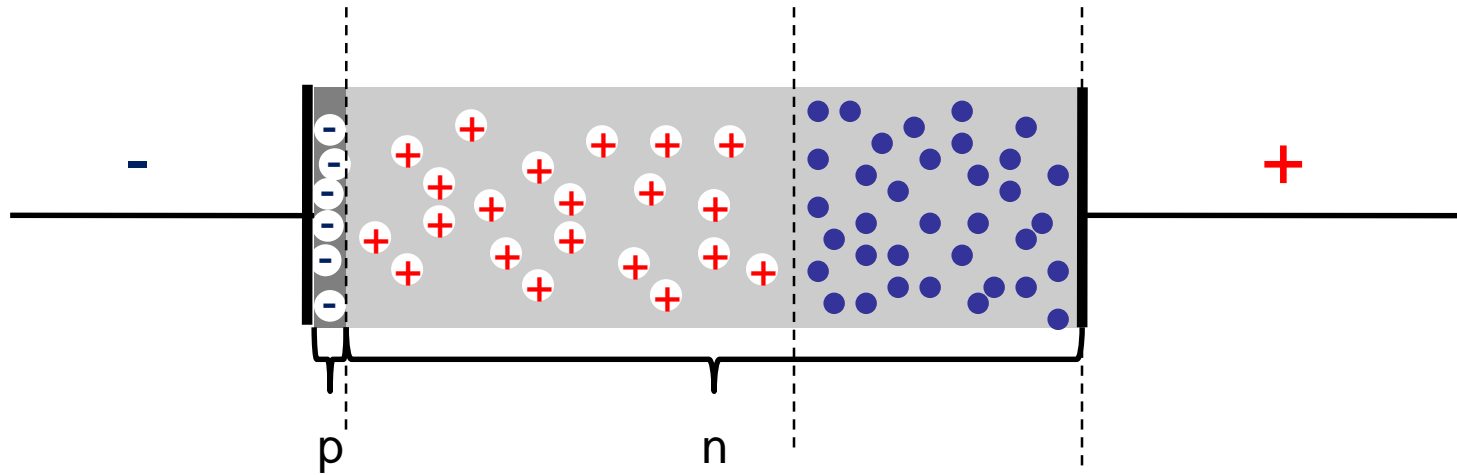
Fully-Depleted Silicon Detector



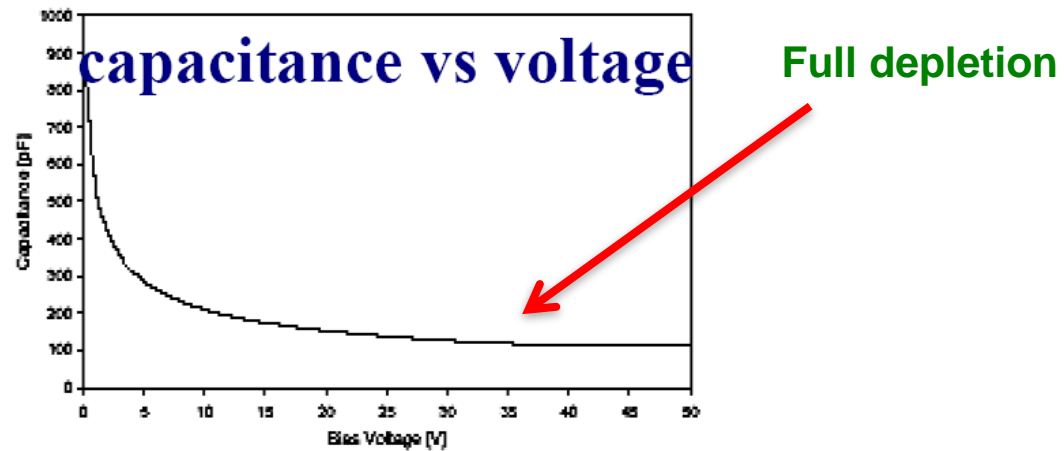
Over-Depleted Silicon Detector



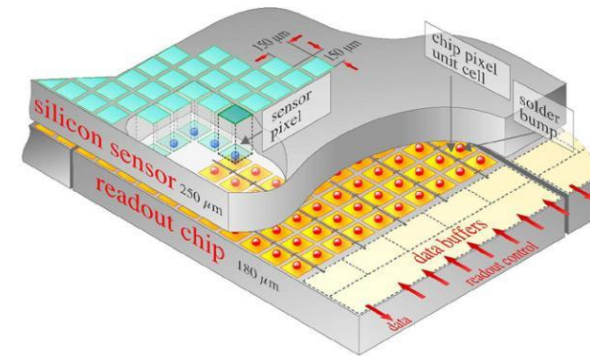
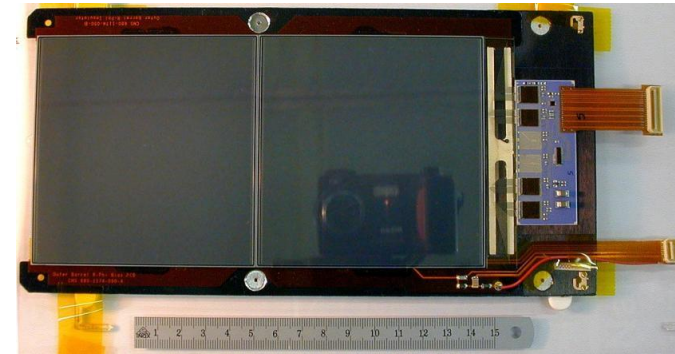
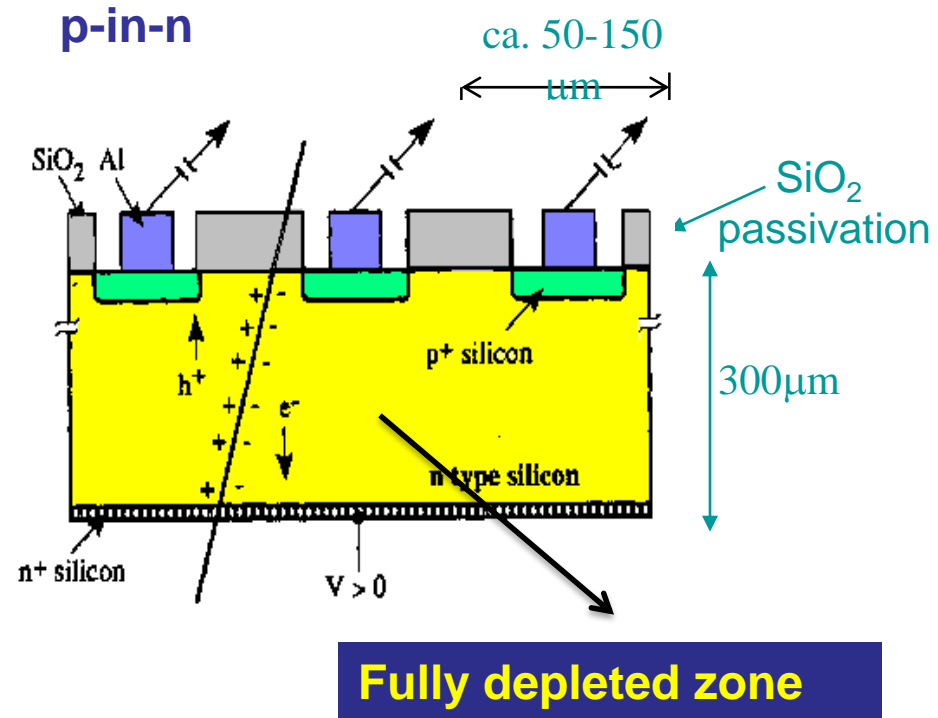
Depletion Voltage



The capacitance of the detector decreases as the depletion zone increases.

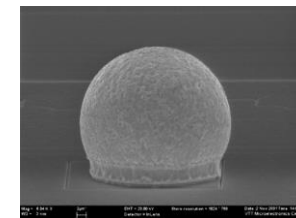
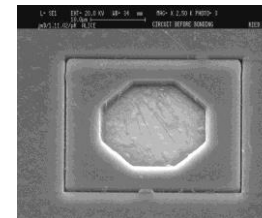


Silicon Sensor



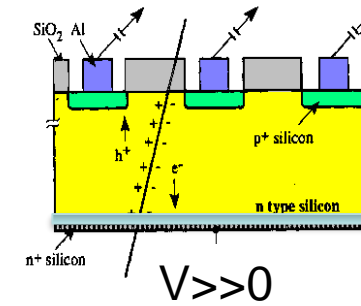
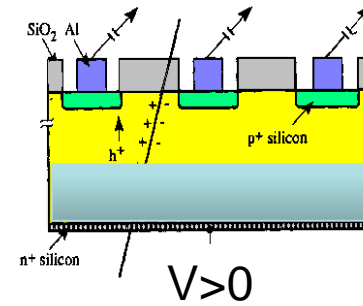
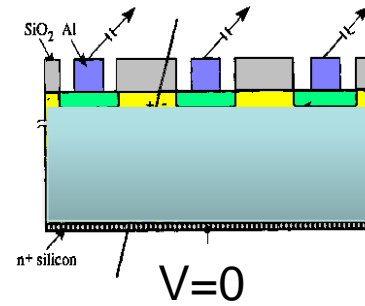
N (e-h) = 11 000/100 μm

Position Resolution down to ~ 5 μm !



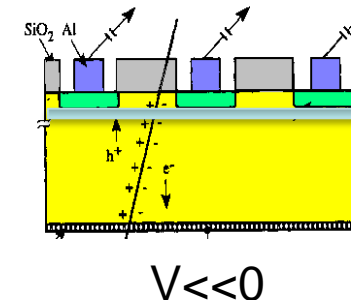
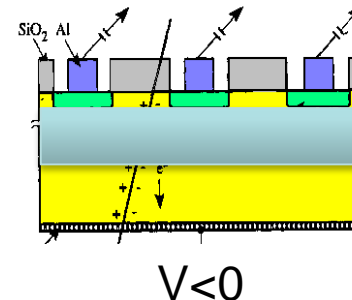
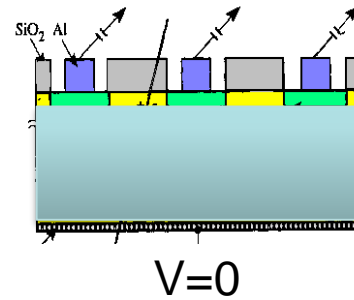
Silicon Sensor before Irradiation

p(strips)-in-n



→ depletion grows from the segmented side

n+(strips)-in-n



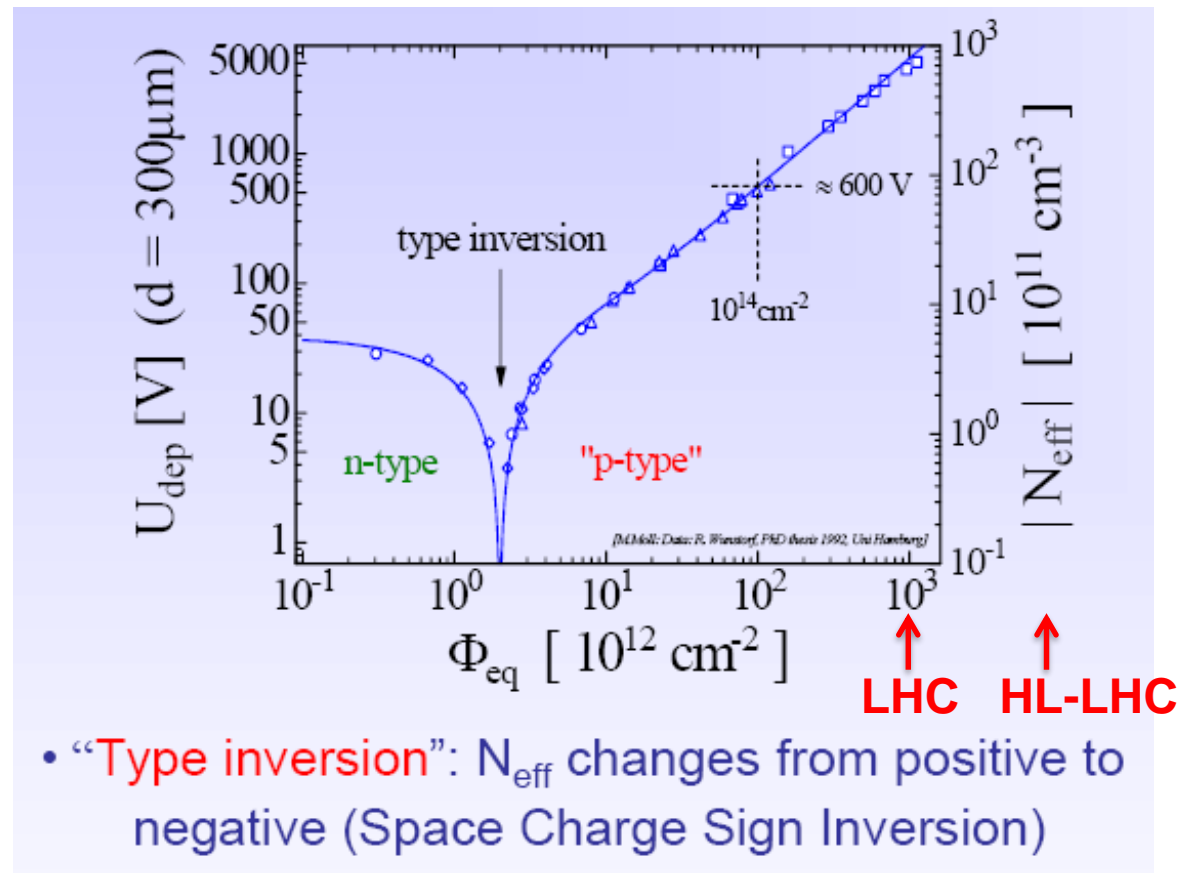
- depletion grows from the un-segmented side
- **This detector does not work properly unless it is fully depleted.**
- For partial depletion the ,charge collection' is very inefficient and the ,cluster size' is increasing.

Radiation Effects, Type Inversion

Type inversion ! An n-type Si detector becomes a p-type Si detector !

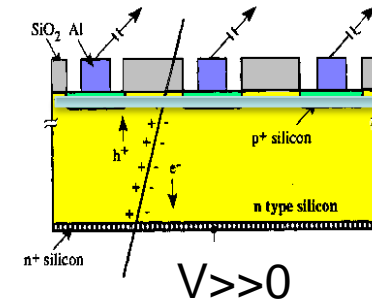
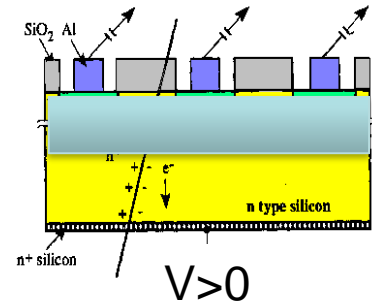
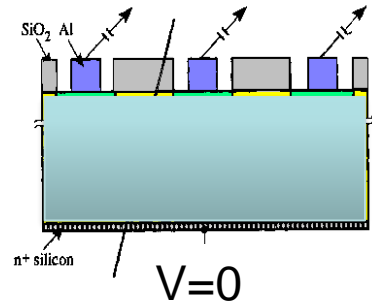
More voltage is needed to fully deplete the detector.

It might happen that the full depletion voltage becomes larger than the breakdown voltage
→ have to work in under depleted regime.

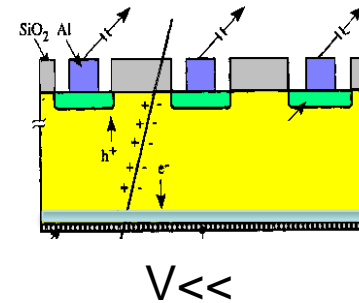
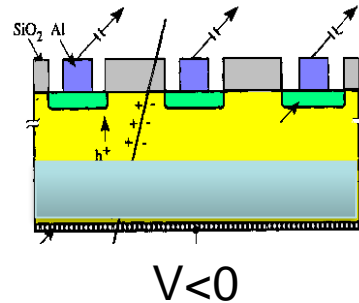
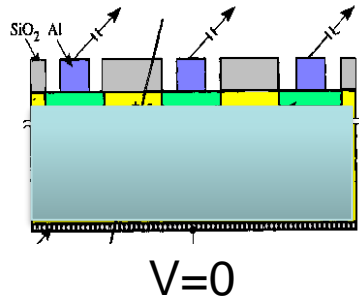


Silicon Sensor after Irradiation and type inversion

p(strips)-in-n



→ depletion grows now from the unsegmented side !



→ depletion now grows from the segmented side
→ can work in under-depleted mode

For high radiation environment, where one might not reach full depletion after some time, n-in-p detectors are preferred.

p-in-n and n⁺-in-n sensors

p-in-n single sided processing

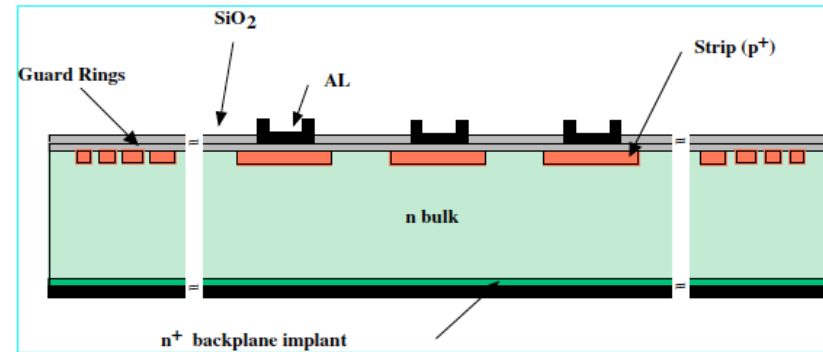


Figure 3.11: Schematic cross section of a p-in-n detector.

n-in-n double sided processing

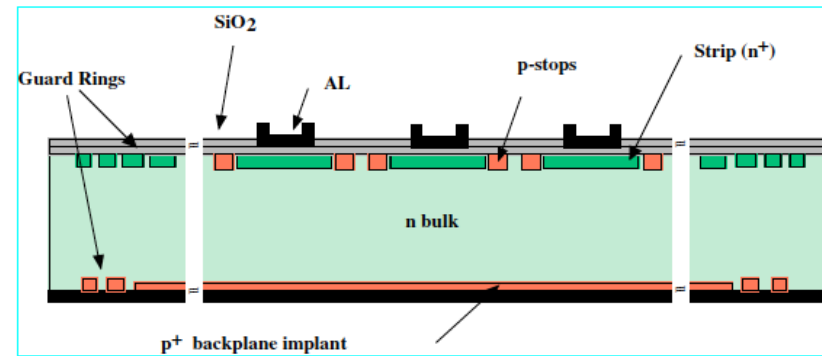


Figure 3.10: Schematic cross section of a n-in-n detector.

from P. Riedler

n-in-p Silicon Sensors

Since recently p-bulk material is available in a quality that is sufficient for these detectors.
Baseline for large areas of HL-LHC trackers !

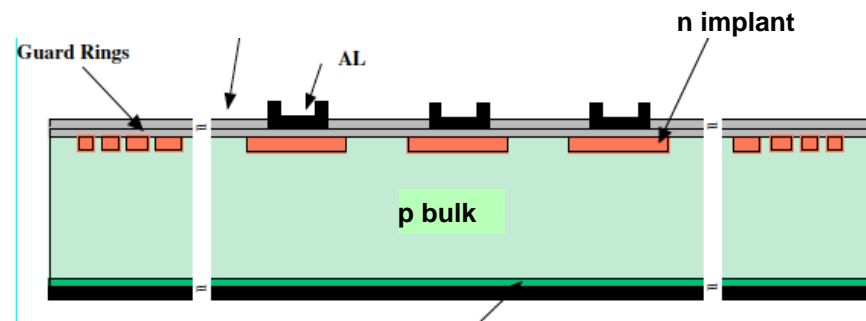
Advantage of n-in-p technology:

No type inversion

Depletion from the 'correct' side (i.e. from the readout side)

Single sided processing is possible

Electrons drift towards the readout side and are trapped less because electrons are faster
→ still good signal after irradiation.



Radiation Effects 'Aging'

LHC Pixels:	10^{15} n/cm ²	14 TeV	300fb ⁻¹
HL-LHC Pixels:	10^{16} n/cm ²	14TeV	3000fb ⁻¹
FCC-hh Pixels:	2×10^{18}	100TeV	30 000fb ⁻¹

First Pixel layer only !! The rest of the tracker volume has significantly less radiation.

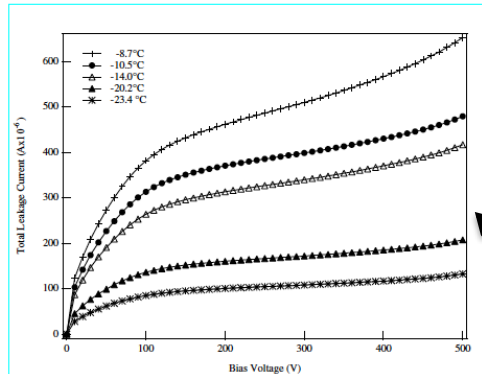
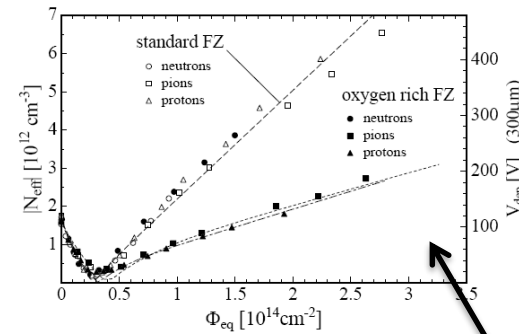
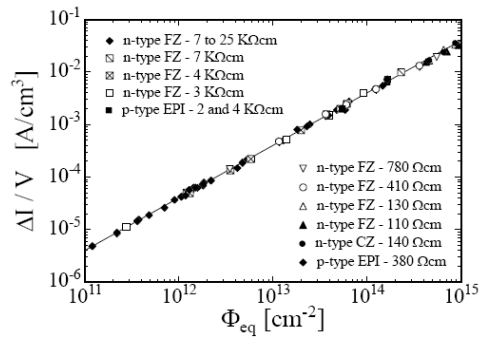
- Two general types of radiation damage
 - "Bulk" damage due to physical impact within the crystal
 - "Surface" damage in the oxide or Si/SiO₂ interface
- Cumulative effects
 - Increased leakage current (increased shot noise)
 - Silicon bulk type inversion (n-type to p-type)
 - Increased depletion voltage
 - Increased capacitance
- Sensors can fail from radiation damage
 - Noise too high to effectively operate
 - Depletion voltage too high to deplete
 - Loss of inter-strip isolation (charge spreading)
- Signal/noise ratio is the quantity to watch

Radiation Effects 'Aging'

Increase of leakage current

Increase of depletion voltage

Decrease of charge collection efficiency due to under-depletion and charge trapping.



Use silicon material engineering to limit radiation damage

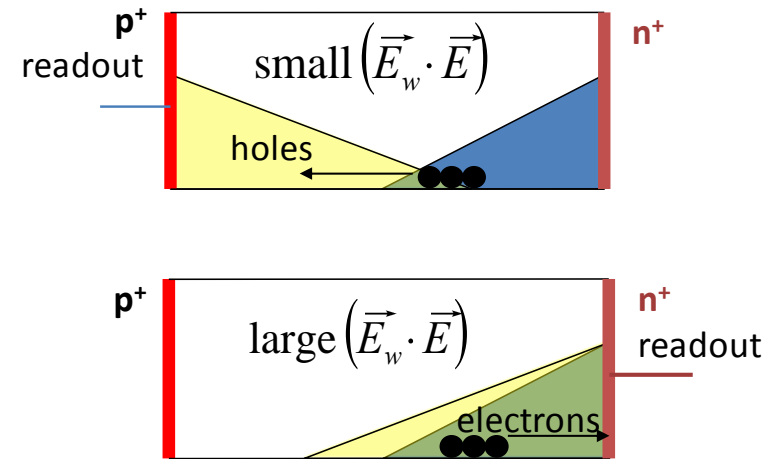
Use cooling to decrease leakage current (approx. factor two every 8 degrees)

from P. Riedler
Figure 3.17: I-V curve of detector Wedge 12-1 at various temperatures after 12 days at 25 °C.

Sensor Technology in Present Experiments

- p-in-n, n-in-p (**single sided process**)
- n-in-n (**double sided process**)
- Choice of sensor technology mainly driven by the **radiation environment**

	Fluence 1MeV n_{eq} [cm ⁻²]	Sensor type
ATLAS Pixel*	1×10^{15}	n-in-n
ATLAS Strips	2×10^{14}	p-in-n
CMS Pixels	3×10^{15}	n-in-n
CMS Strips	1.6×10^{14}	p-in-n
LHCb VELO	$1.3 \times 10^{14**}$	n-in-n, n-in-p
ALICE Pixel	1×10^{13}	p-in-n
ALICE Drift	1.5×10^{12}	p-in-n
ALICE Strips	1.5×10^{12}	p-in-n



G. Kramberger, Vertex 2012

n-side readout (n-in-n, n-in-p):

- Depletion from segmented side (under-depleted operation possible)
- Electron collection
- Favorable combination of weighting field and
- Natural for p-type material

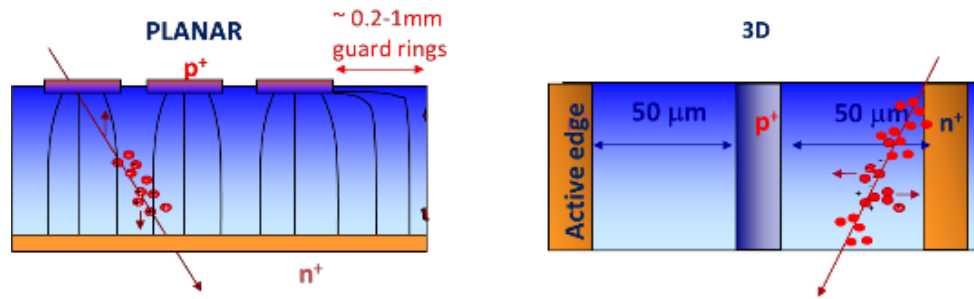
** per year

Key Sensor Issues for the Upgrades

- **Radiation damage** will increase to several $10^{16} n_{eq} \text{ cm}^{-2}$ for the inner regions in ATLAS and CMS
 - Example of common activities to develop radiation harder sensors within the RD50 collaboration
 - Operational requirements more demanding (low temperature and all related system aspects)
- **Increased performance:**
 - Higher granularity
 - Lower material budget
- **Control and minimize cost**
 - Large areas
 - Stable and timely production

Upgrades	Area	Baseline sensor type
ALICE ITS	10.3 m ²	CMOS
ATLAS Pixel	8.2 m ²	<i>n-in-p</i>
ATLAS Strips	193 m ²	n-in-p
CMS Pixel	4.6 m ²	<i>n-in-p</i>
CMS Strips	218 m ²	n-in-p
LHCb VELO	0.15 m ²	<i>n-in-p</i>
LHCb UT	5 m ²	<u>n-in-p</u>

3D Sensors



Both electrode types are processed inside the detector bulk

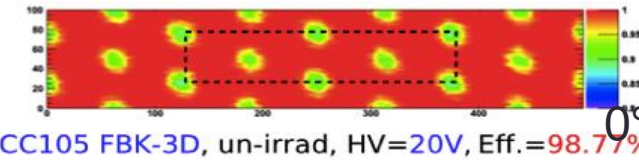
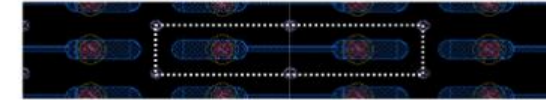
Max. drift and depletion distance set by electrode spacing - reduced collection time and depletion voltage

Very good performance at high fluences

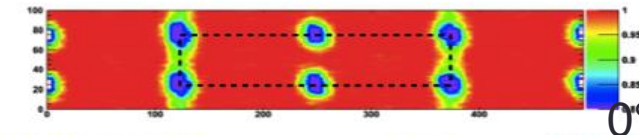
Production time and complexity to be investigated for larger scale production

Used in ATLAS IBL

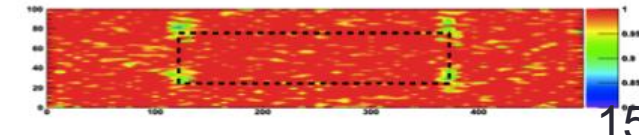
3D pixel sensors



SCC105 FBK-3D, un-irrad, HV=20V, Eff.=98.77%



SCC81 CNM-3D, n-irrad HV=160V, Eff.=97.46%



SCC34 CNM-3D, p-irrad, HV = 160V, Eff.=98.96%

ATLAS IBL Sensor (Threshold: 1600 e
proton-irrad: 5×10^{15} n_{eq}/cm² with 24 MeV protons
neutron-irrad: 5×10^{15} n_{eq}/cm² by nuclear reactor)

From: *Prototype ATLAS IBL Modules using the FE-I4A Front-End Readout Chip*
(JINST 7 (2012) P11010)

CMOS Sensors

CMOS sensors contain sensor and electronics combined in one chip

No interconnection between sensor and chip needed

Standard CMOS processing

Wafer diameter (8")

Many foundries available

Lower cost per area

Small cell size – high granularity

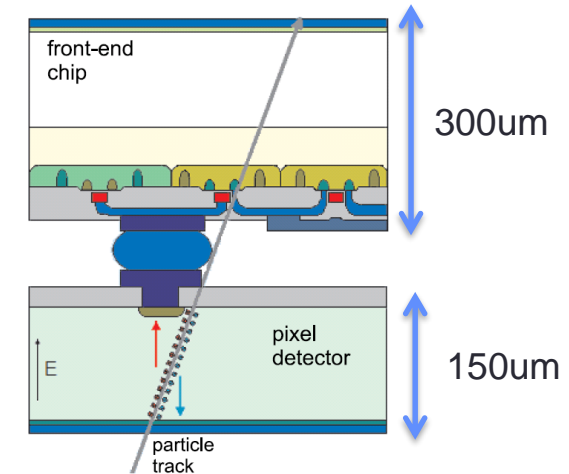
Possibility of stitching (combining reticles to larger areas)

Very low material budget

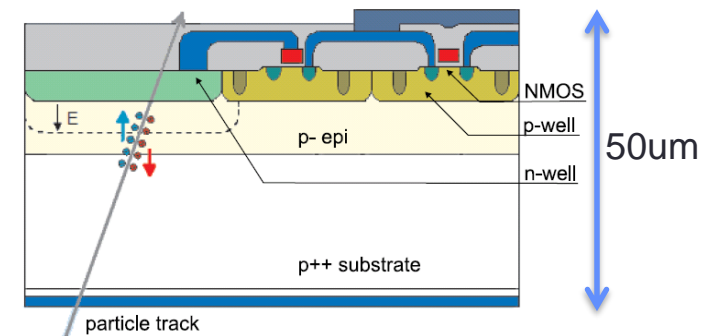
CMOS sensors installed in STAR experiment

ALICE ITS upgrade

Hybrid Pixel Detector



CMOS (Pixel) Detector



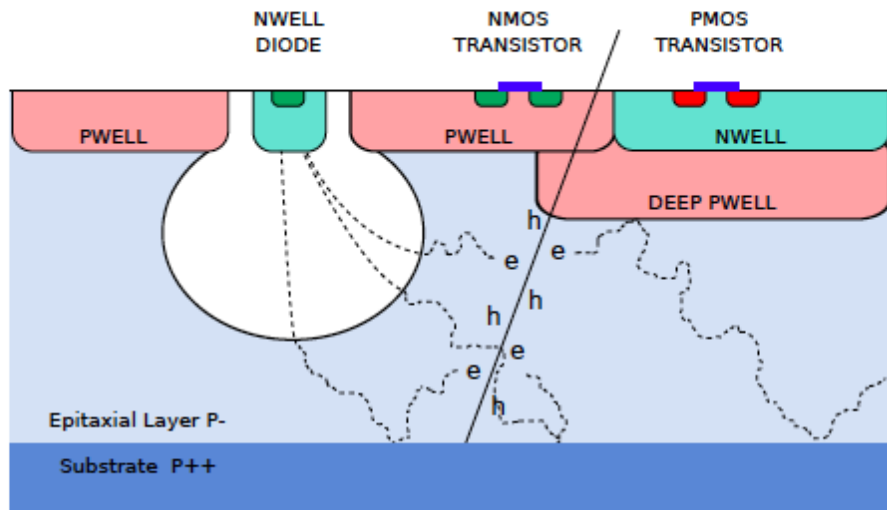
PIXEL Chip - technology

Monolithic PIXEL chip using Tower/Jazz 0.18 μm technology

- feature size 180 nm
- gate oxide < 4nm
- metal layers 6
- high resistivity epi-layer
 - thickness 18-40 μm
 - resistivity 1-6 k $\Omega \times \text{cm}$
- “special” deep p-well layer to shield PMOS transistors (allows in-pixel truly CMOS circuitry)
- Possibility to build single-die circuit larger than reticle size

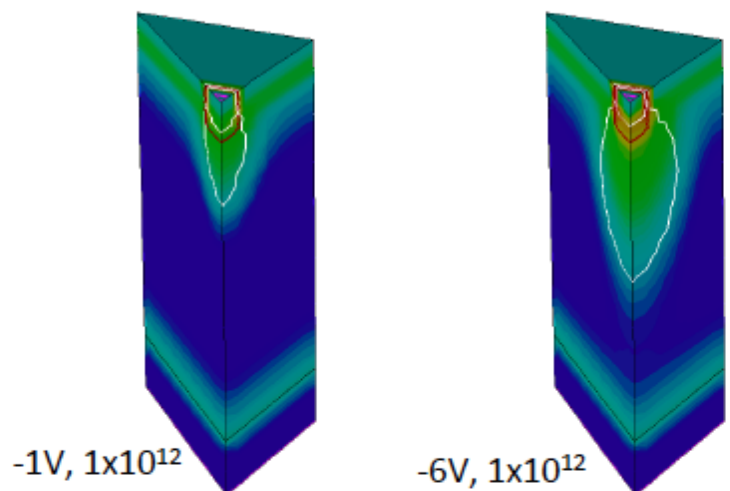
Radiation Resistance (< 10^{13} neq/cm², < 10kGy) and charge collection time (> \approx microseconds) do for the moment not allow application in high rate environments of ATLAS, CMS, LHCb.

But ! Stay tuned for developments in the near future.



Schematic cross-section of CMOS pixel sensor (ALICE ITS Upgrade TDR)

TCAD simulation of total diode reverse bias (ALICE ITS Upgrade TDR)



diode 3 μm x 3 μm square n-well with 0.5 μm spacing to p-well white line: boundaries of depletion region

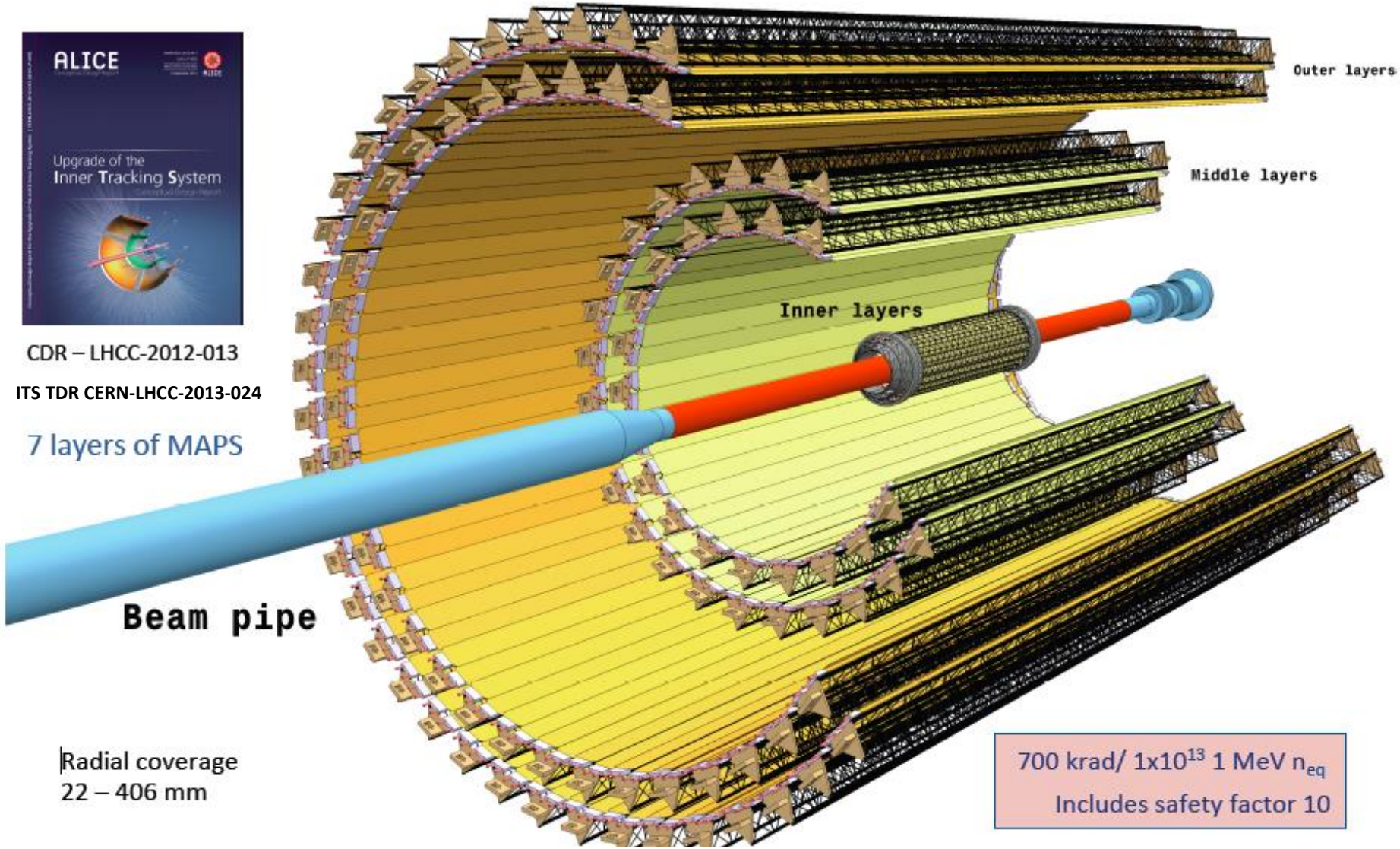
New ITS Layout



25 G-pixel camera
(10.3 m²)



CDR – LHCC-2012-013
ITS TDR CERN-LHCC-2013-024
7 layers of MAPS



Radial coverage
22 – 406 mm

700 krad/ 1×10^{13} 1 MeV n_{eq}
Includes safety factor 10

ALICE ITS upgrade

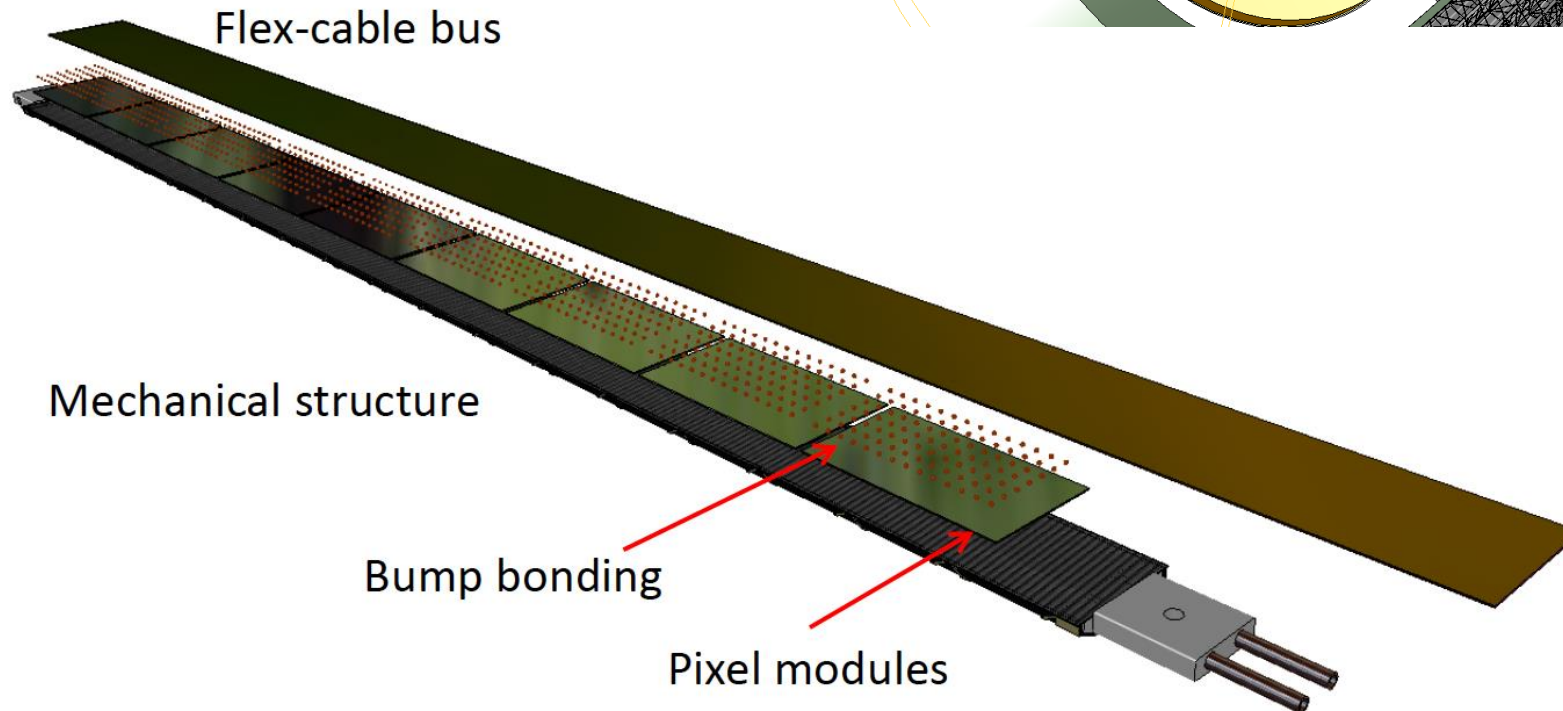
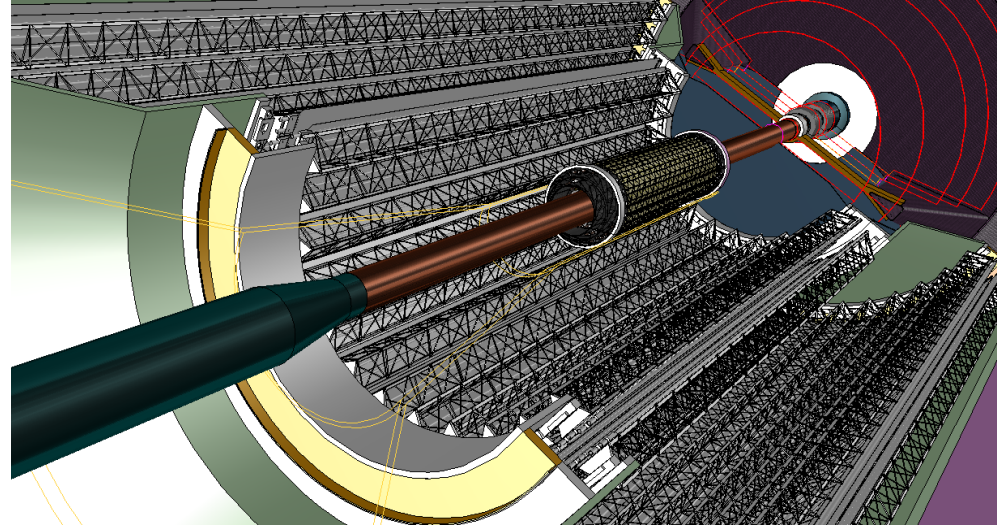


Inner Barrel: 3 layers

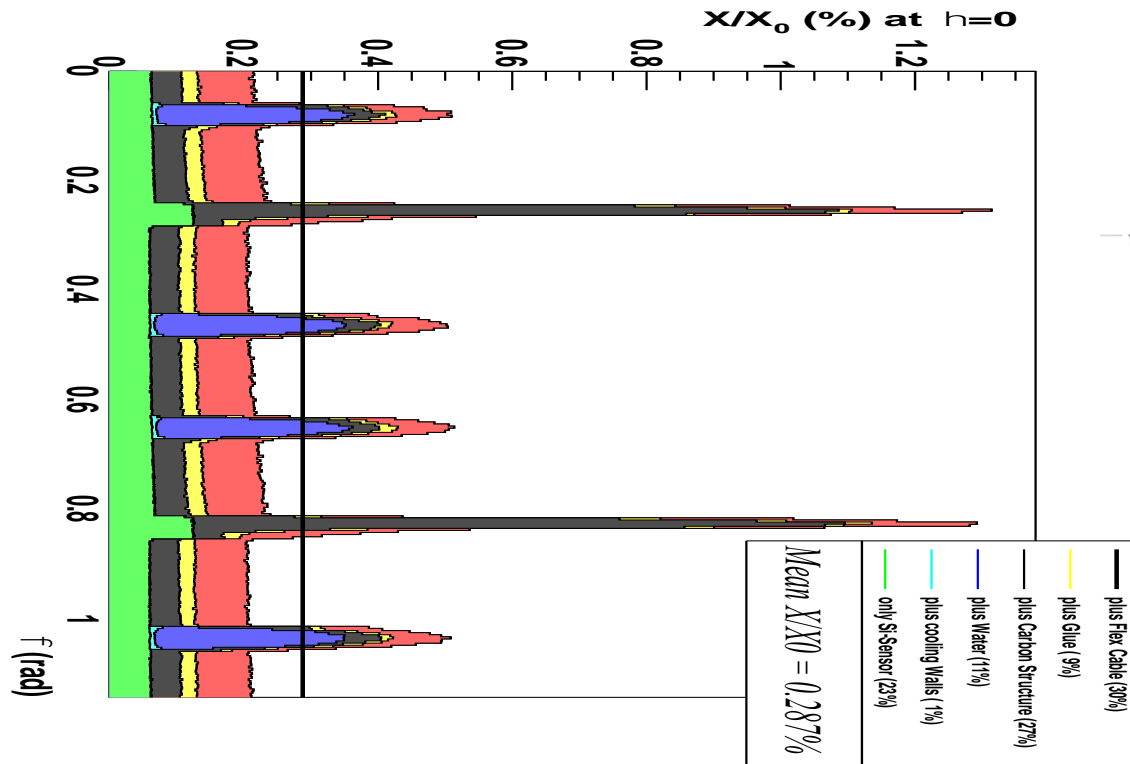
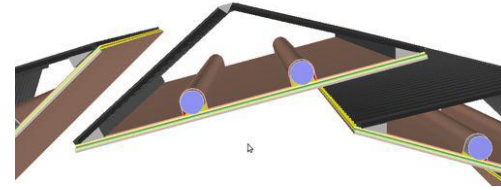
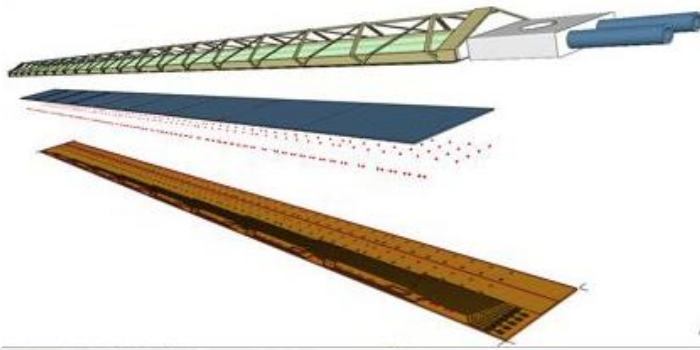
Outer Barrel: 4 layers

Detector module (Stave) consists of

- Carbon fiber mechanical support
- Cooling unit
- Polyimide printed circuit board
- Silicon chips (CMOS sensors)

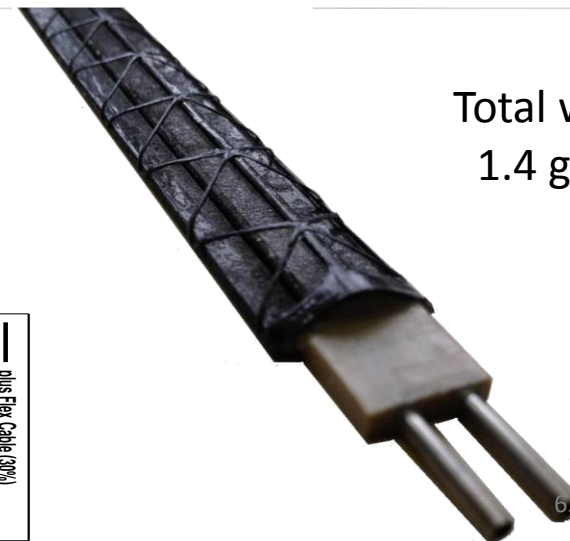


Inner Barrel Detector Stave



MECHANICS & COOLING

✓ Design optimization for material budget reduction



Total weight
1.4 grams

Tracking

Silicon sensors are the key detectors for vertex determination and momentum spectroscopy.

In addition to position resolution, material budget and radiation hardness are the key requirements for silicon trackers.

n-in-p strips sensors and hybrid pixels feature prominently at the HL-LHC.

Monolithic silicon sensors have significantly improved over the last years in terms of speed and radiation hardness and will have a large scale application in ALICE.

